U.PORTO
FEUP FACULDADE DE ENGENHARIA
UNIVERSIDADE DO PORTO
M 2018

Preliminary design of an Achilles tendon scaffold based on a simple model approach

Pedro Alves Douteiro Cranfield Ramalho

DISSERTAÇÃO DE MESTRADO APRESENTADA
À FACULDADE DE ENGENHARIA DA UNIVERSIDADE DO PORTO EM
ENGENHARIA METALÚRGICA E DE MATERIAIS

Orientadores:

Prof. Rui Miranda Guedes
Prof. Maria Ascensão Lopes

CANDIDATO		*Código*
TÍTULO		
DATA	__ de _____ de _____	
LOCAL	Faculdade de Engenharia da Universidade do Porto – Sala _____ - __:__h	
JÚRI	*Presidente*	DEMM/FEUP
	Arguente	DEM/FEUP
	Orientador	DEMM/FEUP

Abstract

Tendons and ligaments are structures that are present through the human body and when damaged, may present considerable complications. Due to their low scarring ability, especially in intraarticular tissues, surgery is frequently required. Surgery that consists in suturing both ends of the injured tissue is ineffective due to the low-quality scarring and the low mechanical properties exhibited by the tissue afterwards. Due to this, autograft techniques are the most common route in tissue repairing surgeries. Despite showing good results, this technique also reveals some disadvantages.

Tissue engineering scaffolds may aid in overcoming these limitations. They consist in an artificial biodegradable ligament or tendon which is implanted in the site of the damaged tissue and promotes tissue growth while it degrades, besides providing mechanical support. Ideally, a tendinous or ligamentous tissue takes its place afterwards. However, designing a scaffold is complex as it must meet some requirements such as being biocompatible, promoting tissue growth, displaying a mechanical behaviour similar to the tissue which is being repaired and more.

The goal of this investigation was to design a scaffold for the regeneration of the Achilles tendon, possessing appropriate chemical composition and mechanical properties during degradation. The design of two types of scaffolds using a simplified model was performed. One fully degradable, and one semi-degradable scaffold were designed utilizing polymers which were already employed in biomedical applications, such as PLGA, PLA, PCL, PDS and PTFE. A structure composed by parallel fibres only and exhibiting a linear elastic behaviour was assumed for the scaffold. To analyse the mechanical behaviour of the scaffold during the regeneration of the tendon, simulations were performed in a spreadsheet. All the data utilized in the design and simulations were gathered from the literature.

In the simulations, the scaffolds exhibited adequate mechanical behaviour during degradation, losing its properties gradually and preventing the regenerating tissue from rupturing. Therefore, the scaffolds have shown, in this preliminary study, that they could perform well at values of constant strain or stress associated with normal locomotion in the Achilles tendon.

Key words: Scaffold, Biodegradable, Tissue Engineering, Achilles tendon, Design, Simulation

Resumo

Os ligamentos e tendões são estruturas que estão presentes por todo o corpo humano e várias vezes são danificadas. Devido à sua baixa capacidade de cicatrização, principalmente em tecidos intra-articulares, a cirurgia é necessária. A cirurgia que consiste na sutura do tendão ou ligamento é ineficaz, devido à cicatrização de baixa qualidade e baixas propriedades mecânicas apresentadas pelo tecido. Devido a isto, a técnica de autoenxerto é a via mais utilizada em cirurgias de reparação de tecidos. Apesar de apresentar bons resultados, esta técnica também apresenta desvantagens.

O uso de dispositivos biodegradáveis sintéticos pode ajudar a ultrapassar estas desvantagens. O *scaffold* consiste em um ligamento ou tendão artificial biodegradável que é implantado no local do tecido danificado e promove o crescimento do tecido enquanto este se degrada, para além de fornecer suporte mecânico. Idealmente, depois da sua degradação, um tecido ligamentoso ou tendinoso toma o seu lugar. Porém, projetar este dispositivo é complexo pois tem que preencher vários requisitos, como ser biocompatível, promover o crescimento do tecido, apresentar um comportamento mecânico adequado, entre outros.

O objetivo deste trabalho foi realizar o *design* de um *scaffold* para o tendão de Aquiles, com uma composição e comportamento mecânico adequado a promover a regeneração do tendão. Utilizando um modelo simples, foi realizado o *design* de dois tipos de *scaffolds*, um totalmente absorvível, e um semi-absorvível utilizando materiais já utilizados em aplicações biomédicas, como PLGA, PLA, PCL, PDS e PTFE. Para o *scaffold*, assumiu-se uma estrutura composta apenas por fibras paralelas, apresentando um comportamento elástico linear. De forma a avaliar o comportamento mecânico durante a regeneração do tendão, realizaram-se simulações numa folha de cálculo. Os dados utilizados neste trabalho foram obtidos através duma análise da literatura.

Nas simulações, os *scaffolds* apresentaram um comportamento mecânico adequado à função, perdendo as propriedades gradualmente e prevenindo a rotura do tecido que se está a regenerar. Os *scaffolds* demonstraram então, neste estudo preliminar, que são capazes de cumprir o seu objetivo enquanto sujeitos a valores de deformação e tensão constantes associados à locomoção normal no tendão de Aquiles.

Motivations and Objectives

Ligaments and tendons have a fundamental role in allowing in the human body keeping bones and muscles together, primarily contributing to the transmission of forces and the stabilization of joints. When these tissues are injured, it has a great impact on the normal function of joints and leading to instability and pain. Injuries in tendons and ligaments also have other major concerns such as their low-quality healing and low healing rates. Some solutions for the repair of these tissues are employed, however several limitations presented by these techniques motivate the research for better solutions in the field of tissue repair. Tissue engineering scaffolds seem a promising approach in tissue repair, however, an optimal solution was not yet found.

In order to further study scaffolds used in the repair of the Achilles tendon, this study focused on determining a chemical composition for the scaffolds and studying its mechanical behaviour during the degradation of the scaffold and regeneration of the Achilles tendon tissue, the load transference from the scaffold to the tissue and whether the scaffold could provide an appropriate mechanical support to the tissue during its regeneration preventing it from rupturing in the earlier stages.

Acknowledgements

Gostaria de expressar a minha gratidão a todos que contribuíram para a realização deste trabalho.

Aos meus orientadores, Professor Rui Miranda Guedes e Professora Maria Ascensão Lopes pela disponibilidade, acompanhamento e apoio durante o decorrer desta investigação.

A todos os professores do Departamento de Engenharia Metalúrgica e Materiais da Faculdade de Engenharia da Universidade do Porto, pela sua dedicação e por serem responsáveis pelo meu desenvolvimento e crescimento académico.

À professora Laura Ribeiro, pela sua gentileza, paciência e apoio constante concedido durante o curso que foi fundamental no meu percurso académico.

À minha família e amigos pela por toda a paciência e apoio revelados, que foram essenciais para a conclusão deste trabalho.

Index

Figures Index:

Tables Index

Abbreviations

ECM – Extracellular matrix

QLV – Quasi-linear viscoelasticity

PGA – Polyglycolic acid

PLA – Polylactic acid

PLGA – Poly (lactic-co-glycolic) acid

PLLA – Poly (L-lactic) acid

PDGF – Platelet rich growth factor

FGF – Fibroblast growth factor

TGF – Transforming growth factor

3D – Three-dimensional

2D – Two-dimensional

FDA – Food and drug administration

LARS – Ligament Advanced Reinforced System

PTFE - Polytetrafluoroethylene

ACL – Anterior cruciate ligament

PET – Polyethylene terephthalate

PUU – Polyurethane urea

ROP – Ring opening polymerization

Tg – Glass transition temperature

Mw – Weight-average molecular weight

PCL – Polycaprolactone

PP – Porcine pancreatic

PDLA – Poly(D-lactic) acid

PDLLA – Poly (D,L-lactic) acid

LA – Lactide

GA – Glycolide

PDS - Polydioxanone

PBS – Phosphate buffer saline

GPC – gel permeation chromatography

Tm – Melting temperature

σ_0 – Initial tensile strength

PGACL – Poly(glycolide-co-ε-caprolactone)

SEM – Scanning Electron Microscopy

DSC – Differential scanning calorimetry

RSA – Roentgen stereophotogrammetric analysis

R^2 – Coefficient of determination

σ_r – Tensile strength

E – Young's Modulus

A – Cross-section area

P – Load

σ – Tension

ε – Strain

V – Volume fraction

Nf – Number of fibres

Pmax – Maximum load

A0 – Initial cross-section area

Pef – Effective load

EA – Young's Modulus x Cross-section area

S – Stiffness

L - Length

1. Introduction

Ligaments and tendons are an essential part of the musculoskeletal system, primarily contributing to the transmission of forces and the stabilization of joints. Ligaments have two insertions, connecting bone to bone, while tendons have only one insertion, having the other joined with the muscle. Both are connective tissues, consisting in dense bands of collagen fibres, named fibrous connective tissue. They can vary in shape, orientation and size [1]. This makes performing simple and complex motions possible. Tendons aid in motion of the body by transmitting force from the muscle to the bone. These tissues have high mechanical strength under tensile loads and are resistant to cyclic efforts that are executed during the daily activity of the musculoskeletal system as they work as elastic energy absorbers [2, 3]. Knowing this, damaging these tissues has a great impact in normal biomechanical function impairing the function of joints and may lead to the degeneration of joints and abnormal wear, as well as instability and pain. Injuries in ligaments and tendons are very common, especially for people involved in sports activities and elderly people. There are many areas throughout the body where these tissues can experience such injuries, like knees, hips, shoulders, ankles, elbows and wrists [3-5].

The incidence of tendon injuries has increased substantially in the last decades, particularly in athletes. The number of Achilles tendon injuries heavily influences this increase in tendon problems. Due to its limited blood supply, an injured Achilles tendon, especially in ruptures, heals slowly. This limited healing capacity complicates the treatment for this tissue. Spontaneous healing may happen, but it generally results in the formation of scar tissue which possesses low mechanical properties. Surgically, the simplest solution is the suturing of both ends of the tendon. Another approach used is the implantation of allo- or autografts. These yield better results than the suture surgery, but still exhibit disadvantages such as donor site morbidity, limited availability, disease transmission and tissue rejection [6, 7]. Along with these options, the use of synthetic non-degradable ligament replacements was also employed, such as the Gore-Tex® artificial ligament and the Dacron ligament. However, they revealed poor long-term results [8].

Therefore, tissue engineering represents a more promising approach as it combines knowledge and strategies from material science, molecular biology, medicine and

engineering to enable full tissue regeneration rather than replace the injured tissue with one partially functionalized foreign substitute. Tissue engineering generally includes a porous, three-dimensional, biodegradable scaffold which behaves as a temporary support that enables tissue growth. This structure enhances tissue growth by aiding in cell proliferation, promoting matrix production and organizing the matrix into functional tissues. Additionally, there are scaffold enhancing approaches which increase the scaffold's performance and further promote tissue growth. These approaches include cellular hybridization, surface modification, use of growth factors and mechanical stimulation [7, 9].

The porous scaffold must be biodegradable, biocompatible, have the appropriate mechanical properties for the applications, the architecture should be optimal, providing enough area for cell attachment, and proliferation and the degradation rate must be suitable, in order for when the tissue is healed, the scaffold be completely degraded [10]. To this day, many materials have been investigated for use in scaffolds for tissue engineering. These include synthetic polymers (polyurethane, polylactic acid, polyglycolic acid, polycaprolactone, polyhydroxyalkanoates and alginates), fibrin, hydrogels, silk and other biological materials [11].

2. Tendons and Ligaments

2.1. Ligament and Tendon Structure

While ligaments and tendons appear as a single structure, they are in fact a complex system composed by smaller components. Both tendons and ligaments have a very similar structure. The main cell type present in these tissues are fibroblasts. Fibroblasts present in tendons are elongated and are named tenoblasts. These are immature tendon cells which will give rise to tenocytes. Tenocytes are terminally differentiated tendon cells with limited proliferative capacity and are attached to collagen fibres throughout the tissue. They are connected to the ECM (Extracellular matrix) by integrins that allow cell to sense and respond to mechanical stimuli. These integrins are transmembrane receptors that enable cell-ECM adhesion. These cells secrete a precursor of collagen, named procollagen, which is then cleaved into collagen fibres. Fibroblasts only represent a small portion of the tissue. Water constitutes most of the tissue's composition (70% wet weight), being responsible for

cellular function and viscoelastic behaviour. For the solid components, collagen type I is the main component, representing 65-80% of the dry mass. This type of collagen constitutes 95% of the collagen content, with the remaining 5% being collagen types III, VI, XI and XIV). Other constituents comprise the remaining percentage such as elastin, actin, laminin and proteoglycans which are responsible for storing water, bridging the gap between neighbouring fibres and providing shear resistance [1, 12].

Table 1 - Biochemical constitution of tendon (wet weight)

Tissue type (wet weight)	Water (%)	Collagen (%)	Collagen type I (%)	Other types of collagen (%)	Other components (%)	Ref.
Tendon	70	20-24	19-23	1	6-10	[10,11]

The tendon has a hierarchical structure with different levels of organization including collagen molecules, fibrils, fibres, and fascicles which are parallel to the long axis of the tissue. In Figure 1 these components are illustrated. Tendinous and ligamentous structures are very similar but have some differences. Tendons have less percentage of proteoglycans in their structure, and they have slightly more percentage of collagen fibrils and more organized [1]. Microscopically, it is possible to observe that ligaments and tendons display a “waviness” in their structure that explains their mechanical behaviour, this characteristic of the structure is called “crimp”. The angle and length of the crimp pattern varies on whether it is a tendon or a ligament, its anatomical site and its location in the tissue. Looking at the mechanical behaviour of these tissues, it is possible to understand that this crimp has a major role on the non-linear viscoelastic behaviour [13, 14].

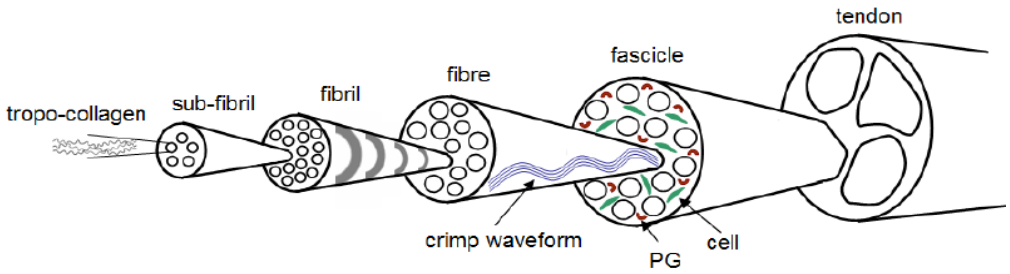

Figure 1 - Hierarchical structure of tendons (adapted from [15])

2.2. General overview of the mechanical behaviour of tendons and ligaments

Soft tissues like ligaments and tendons display a time-dependent behaviour. This means that the relationship between stress and strain is not constant but rather depends on the time displacement or load. This behaviour can be observed when the tissue is under cyclic loading. There are three major characteristics of a viscoelastic material: Creep, stress relaxation and hysteresis. An example of the viscoelastic, or time-dependent behaviour of tissues, is when the tissue is held at a constant strain level, the stress in the tissue decreases with time. This phenomenon is known as stress relaxation (Figure 2) [1, 16].

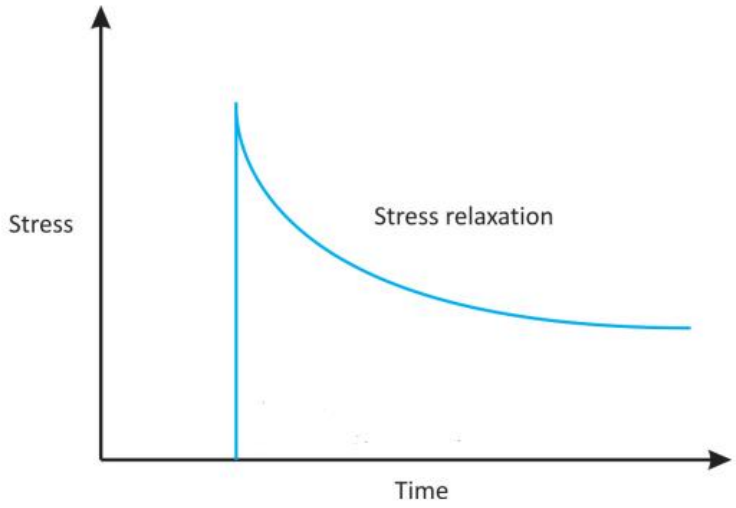

Figure 2 - Example of stress relaxation at constant deformation (adapted from[1])

Also, if the tissue is held at a constant stress level, the strain in the tissue increases with time, which is known as creep (Figure 3). Creep does not take place in normal elastic materials since the material, under a constant load, does not elongate independently of how long the load is applied. This behaviour is thought to be a function of the main component, collagen as well as the other components such as proteoglycans, glycoproteins, elastin and water. Another characteristic of the behaviour of these tissues is hysteresis or energy dissipation. When a viscoelastic material is loaded and unloaded, the loading curve is different than the unloading curve, as can be seen in Figure 4. This is called hysteresis. The difference between the two curves forms a hysteresis loop and represents the amount of energy dissipated during loading. This energy is lost as heat [1].

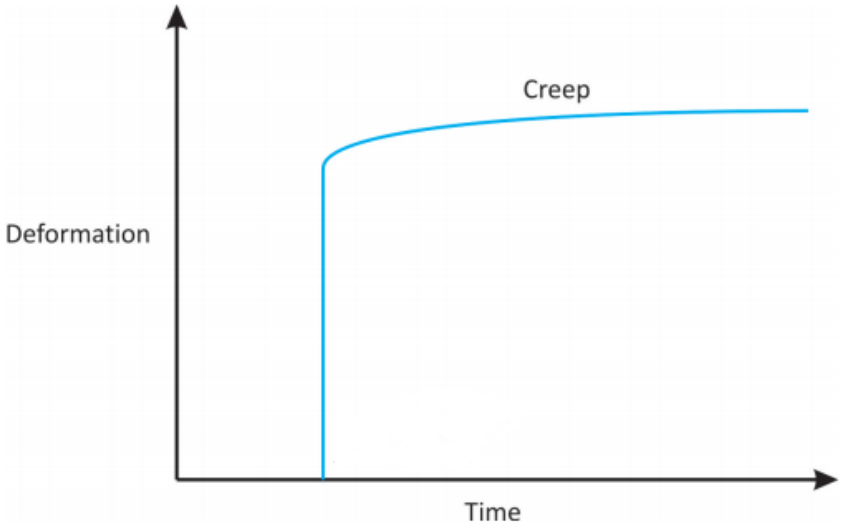

Figure 3 - Example of creep at constant stress (adapted from [1])

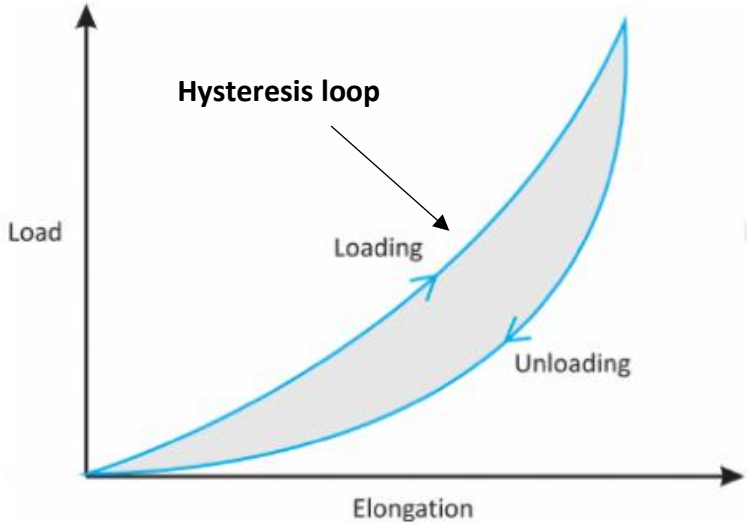

Figure 4 - Example of Hysteresis (adapted from [1])

These viscoelastic behaviours for tendons and ligaments are essential for securing the motion and activity of the human body preventing fatigue failure of those tissues. For example, during walking or jogging, cyclic stress relaxation occurs, in which the maximum stress in the tissue decreases with each cycle [17].

To describe the viscoelastic behaviour of ligaments and tendons mathematical models have been made. Many have been used but the most commonly used model in biomechanics literature is the QLV (quasi-linear viscoelastic) theory. It was modified and adopted to describe the viscoelastic properties of ligaments and tendons. This theory was used to join the nonlinearity (dependence of properties on load or strain) and time dependence (viscoelasticity) in a simplified integral model. In this model the stress-strain response is described as a separable function consisting of a stress or strain dependent function (independent of time) and a time dependent

relaxation or creep function (independent of stress or strain). Although, the QLV theory was frequently used to describe viscoelastic behaviour, only few studies have used it to predict the overall stress-strain response of ligaments and tendons. This is due to the limited ability of the QLV theory to predict the stresses and strains in response to loading conditions other than those used to fit the model. The accuracy of the model is lower at high levels of strain [17, 18]. Funk et al. used the QLV to model the behaviour of foot ligaments and it was adequately modelled until 15% strain [19]. Another limitation of the QLV theory is that it cannot account for creep and relaxation rate dependency and cannot interrelate creep and relaxation [17, 18].

Ligaments display a triphasic behaviour when exposed to strain, as shown in Figure 5. First, there is a region where the tissue presents low amount of stress per unit strain, called non-linear or toe region. In this stage, the force is transferred to the collagen fibrils resulting in the straightening of the crimp pattern. This "uncrimping" presents a lower resistance than when the force is applied to stretch the collagen molecules in the second region, which explains why this region of the stress-strain curve shows relatively low stiffness. As the collagen fibrils become uncrimped, the collagen fibril backbone begins to be being stretched itself, exhibiting a much stiffer behaviour. This can be observed in the second region of the stress-strain curve. In this linear region, the collagen triple helix is stretched and interfibrillar slippage occurs between crosslinks. In the last stage, the individual fibrils start failing by defibrillation, damage accumulates, and stiffness starts to decrease until the whole tissue fails and disrupts [1, 5].

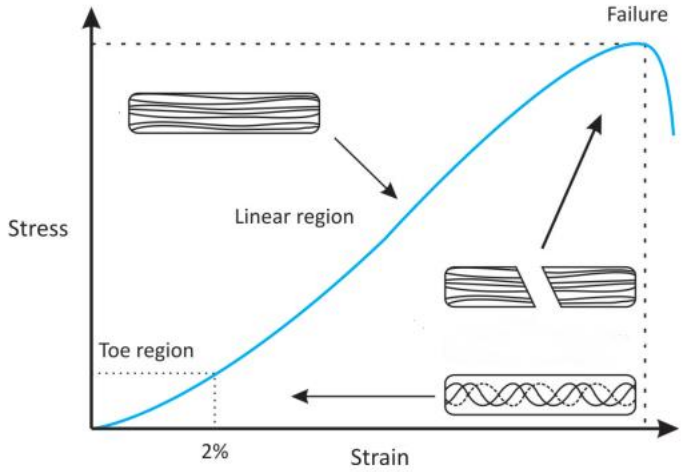

Figure 5 – Illustration of a ligament or tendon stress-strain curve (adapted from [1])

2.3. The Achilles Tendon

The Achilles tendon is the largest and strongest tendon in the human body. Due to its size and functional demands, the Achilles tendon is susceptible to acute and chronic injuries and is directly or indirectly implicated in many pathological conditions of the ankle or foot [20]. During walking, the tendon is subjected to peak forces of 2.2-2.7kN associated with elongations between 14.3-15.2mm [21].

Elastin and collagen are the main constituents of the extracellular matrix of the Achilles tendon, 2 and 70% of the dry weight, respectively. Tenocytes (specialized fibrocytes) and tenoblasts lie between collagen fibres along the long axis of the tendon and represent 90-95% of the cellular elements of the tendon, and chondrocytes, vascular cells, synovial cells and smooth muscle cells constitute the remaining 5-10% [22, 23]. The collagen fibres are packed in parallel bundles which contain nerve, blood and lymphatic vessels, forming fascicles. The fascicles are surrounded by endotenon, which is a fine layer of connective tissue and grouped together, they form the macroscopic tendon. The tendon is surrounded by the epitenon, which is surrounded by the paratenon. These two are separated by a thin layer of fluid that reduces friction during motion [22].

Although the normal Achilles tendon consists almost entirely of type-I collagen, a ruptured Achilles tendon contains a substantial amount of type-III collagen [24]. This is due to the tenocytes that are present in the ruptured Achilles tendon produce more type-III collagen that tenocytes from a normal tendon. As type-III collagen is less resistant to tensile forces, consequently, the mechanical properties of the tendon decrease as well. The healthy Achilles tendon also presents a well-organized cellular arrangement, while the injured Achilles tendon does not [23].

For the regeneration of the tendon, the process occurs in three stages. In the inflammatory phase, erythrocytes and inflammatory cells, such as neutrophils, arrive at the site of the injury. In the first twenty-four hours, macrophages and monocytes predominate and phagocytosis of necrotic materials takes place. Chemotactic factors such as vasodilators and proinflammatory molecules that attract inflammatory cells from surrounding tissue are released. Tenocytes start migrating to the injury site and collagen type-III synthesis begins [25]. In the proliferative phase, the recruitment of tenocytes and its rapid proliferation continues, and the synthesis of proteoglycans,

collagen, especially collagen type-III, and other constituents of the ECM peaks. Initially, these components are arranged in a random manner within the ECM. In the end of this phase, the tissue is highly cellular [7]. After six to eight weeks, the remodelling phase begins, and there is a decrease in cellularity, matrix synthesis and collagen type-III as opposed to the type-I collagen synthesis which increases. This phase can be divided into a consolidation and maturation stage. In the first stage the tissue changes from cellular to fibrous. Tenocyte metabolism remains high and type-I collagen fibres become organized along the tendon axis and are responsible for the mechanical strength of the tissue. As the mechanical properties of the tissue increase, the callus transverse area gradually decreases. However, the tissue remains hypercellular and with high amounts of type-III collagen which has less potential for cross-linking the fibres than type-I collagen, and the collagen fibrils become thinner, leading to inferior mechanical properties when compared to the uninjured tendon. This is represented in Figure 6. After ten weeks, the maturation stage begins, and interaction between collagen structural units lead to higher tendon stiffness and tensile strength and the fibrous tissue gradually changes to scar-like tissue over the course of one year [7, 25].

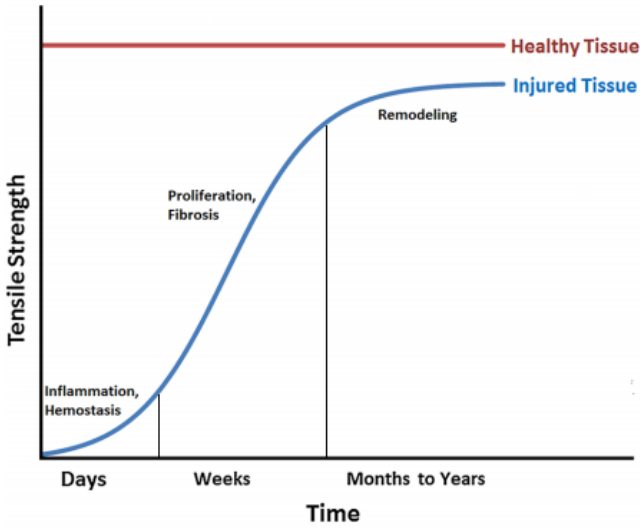

Figure 6 - Representation of the recovery of properties in healing tendons (adapted from [6])

2.4. Current treatment and rehabilitation procedure for Achilles tendon rupture

Achilles tendon ruptures are common, but the treatment of acute ruptures in the Achilles tendon is a topic which is considerably debated as there is no standard protocol for the treatment [26]. The treatment options for the Achilles tendon

rupture include nonsurgical and surgical procedure. In the case of a nonsurgical procedure, a cast-boot will be used with the foot placed in plantar flexion, and early physiotherapy can be performed. As for the surgical procedure these include slightly invasive, open and percutaneous repair of the tendon. Advocates for the nonsurgical treatment defend that by keeping the foot in plantar flexion is enough to achieve healing of the injured tendon. In theory, this healing is achieved without the risks inherent to the surgical procedure. However, Achilles tendon repair surgery is performed due to higher rerupture rates being associated with the nonsurgical treatment. In the meta-analysis conducted by Soroceanu et al., it was suggested that the rerupture rate of both treatments were equivalent [27].

Whether surgical or nonsurgical treatment is applied, they are followed by a rehabilitation period in which the ankle is casted or braced for 6 to 8 weeks. The rehabilitation can involve either immobilization or early mobilization. Immobilization achieves tendon healing by haematoma formation, collagen proliferation and then collagen maturation. However, this method is associated with joint stiffness, muscle atrophy tendocutaneous adhesions [28].

Wolff's law and Davis' law are two major physiological principles in the field of physical rehabilitation, that support early mobilization. They state that bone (Wolff's Law) and soft tissues (Davis' Law) regenerate according to the manner that they are stressed. Davis' Law states that the healing soft tissue responds to stress by reacting along the lines of the given stress. For optimum healing, the tissue should be gradually stressed in order to accept a given force. If the healing tissue is not stressed in the manner required of it previously, the tissue will not be prepared to fully accept preinjury requirements. However, if the regenerating tissue accepts this stress during healing, it will lead to the strengthening of the tissue [29]. Following Davis' Law, the "stretch-hypertrophy rule", from Frost, states that "*Intermittent stretch causes collagenous tissues to hypertrophy until the resulting increase in strength reduces elongation in tension to some minimum level*" [30].

The positive effects of the mechanical load on the remodelling of tendons have been observed [31]. Other studies reported that cyclic tensile loading promotes the collagen fibres to align parallel to the longitudinal axis of the tendon, which inhibits adhesions around the tendon and increases tendon strength, vascularity and number

of collagen fibres [28, 32]. Nöth et al. demonstrated that mechanical stimulation increases collagen production by applying cyclic stretching for 8h per day to a collagen type I matrix. An increase of gene expression of collagen type I and III, fibronectin and elastic in the stretched constructs was observed when compared to the non-stimulated constructs [33].

3. Scaffolds for ligament and tendon regeneration

3.1 Fundaments and requirements

Many tissues in the body are capable of self-healing after injury, but other such as ligaments and tendons have limited regeneration. For this, tissue engineering offers alternative methods to restore tissues and its functions. Scaffolding in tissue engineering consists on the use of a scaffold as a structural support and providing a microenvironment which enables cell attachment, proliferation, and differentiation, in order to produce a functioning tissue to replace or repair a damaged tissue. For that reason, the physical structure, chemical composition and biological attributes are essential features in tissue engineering. These structures should partially mimic the ECM of the tissue which is to be regenerated [10, 11].

For application in tissue engineering, scaffolds have some basic requirements:

- Architecture: they should have open porous interconnected networks for cell nutrition, proliferation, and migration, new tissue formation and vascularization. This porosity is essential but should not compromise mechanical properties [10, 34];
- Biocompatible: The scaffold should be biocompatible by not inducing any harmful, toxic or immunologic response. Also, it should promote cell attachment, growth and differentiation during both *in vitro* culture and *in vivo* implantation [10];
- Mechanical properties: Scaffold should provide mechanical and shape stability to tissue, without provoking stress-shielding. The intrinsic mechanical properties of the biomaterials used in the production of the scaffold should match the properties of the host tissue [23]
- Surface area: The scaffold should provide enough surface area for cells to attach and proliferate [10];

- Biodegradability: The scaffold should be biodegradable and degrade gradually to allow a controlled exposure of the neotissue to the local mechanical environment promoting a structure formation and function more similar to the native tissue. The degradation rate should approximately match the growth rate of the neotissue to avoid the stress shielding phenomenon and allowing room to the new tissue to grow [6].

For various applications inside tissue engineering, the primary materials for scaffolding are polymers. Synthetic polymers have advantages over natural polymers as they are more flexible, their behaviour is more predictable, and have better processability. Physical and chemical properties of these polymers can be easily modified so mechanical and degradation characteristics can be altered. Synthetic polymers such as PGA (Polyglycolic acid), PLA (Polylactic acid) and their copolymer PLGA (Poly (lactic-co-glycolic) acid) are aliphatic polyesters which are frequently used in tissue engineering. These polymers degrade through simple hydrolysis which is desirable as the degradation rates have low variations from host to host, except for cases where inflammations, implant degradation and other complications take place. These materials will be more deeply investigated further in this work [35, 36].

Naturally derived polymers have also been used in tissue engineering such collagen, glycosaminoglycan, alginic acid, chitosan, polypeptides, silk and more. Natural derived polymers often possess highly organized structures and may contain an extracellular substance called ligand, which can be bound to cell receptors. The great advantage of these materials is their biocompatibility however, they are limited by the lack of large quantities and difficulty in processing these materials into scaffolds [36, 37]

One of the vital aspects in the use of a scaffold for tissue regeneration is its mechanical behaviour. The design of the scaffold must meet some requirements such as tensile strength, stiffness and absorption rates which must be appropriate to the injured tissue. The tensile strength of the tissue should be greater than *in vivo* peak loads supported by the tissue as a measure to ensure that the scaffold will not fail under normal conditions. The stiffness of the tendon should be adjusted to the tissue allowing load sharing across the repair site to promote optimal biologic repair and

providing reinforcement at the same time. Also, the scaffold should not stretch more than the toe region of the stress-strain curve [38].

3.2 Scaffold enhancing approaches

Even though tissue engineering scaffolds have a great potential for tissue regeneration and enhancing its properties, many times the structure alone is not enough. Therefore, scaffold enhancing approaches are available.

These include surface modification, growth factor and cell seeding in the scaffold matrix and mechanical stimulation. As said before, the scaffold must interact positively with cells to promote tissue growth. This positive interaction is achieved by creating a microenvironment favourable for cell differentiation and proliferation. The components which enable the creation of this microenvironment include the presence of growth factors, cell-cell interaction and cell-matrix adhesions [39]. Cell adhesion is essential to this process as cells need a substrate to adhere before differentiation and proliferation. However, synthetic polymers do not possess natural binding sites, therefore cell adhesion is mediated through plasma/serum proteins adsorbed into the polymer surface [40]. The parameters which are involved in cell adhesion are surface roughness, chemical composition, the electric charge effect, surface hydrophilicity or hydrophobicity and surface wettability [41]. Knowing this, it is fundamental to identify what are the options to increase the cell adhesion of a scaffold. Surface modification has shown great results in improving cell attachment. It is possible to modify a hydrophobic surface, chemically or physically, into a hydrophilic one manipulating its surface energy. Boland et al. reported an increase in the biocompatibility of PGA fibres through a pre-treatment using concentrated hydrochloric acid [42]. Yang et al. also modified the surface of PLLA (Poly L-lactic acid) and PGA scaffolds but using an anhydrous ammonia plasma treatment and the results showed an improvement in hydrophilicity and surface energy. Cell culture results suggested that the treatment increased cell affinity in the scaffolds [43]. In addition to surface modification, the use of nanofibrous scaffolds can also increase cell adhesion. This technique consists in producing a biomimetic structure that replicates the natural ECM to the nanometre scale. These scaffolds are formed by nanofibers with diameters close to the collagen fibres in the tendon to which cells attach and organize themselves around. These scaffolds have a higher surface area to volume ratio than microfibrous scaffolds [44]. Woo et al. reported that using a

nanofibrous architecture in a scaffold improves protein adsorption, and consequently cell interactions with scaffolds [45].

In tissue engineering scaffold, cells seeding in the scaffold matrix in order to promote the repair of the damaged tissues is also performed. The introduction of cell in scaffold matrixes is known to increase tissue growth and its properties. Young et al. studied the effect of using MSC-seeded implants on the healing of a gap defect on the Achilles tendon of rabbits. Treated tissues showed substantial increase in mechanical properties, cross-section area and better collagen fibre alignment [46]. There are several types of cells which are used in tissue engineering. Studies are still being conducted trying to determine which is the best type of cell for use in tissue engineering [47, 48]. Tenocytes are one obvious option to use in tissue engineering constructs, since they are the primary cell-type in tendons. Cao et al. used a tenocyte seeded PGA scaffold to bridge tendon defects in hens. The tissue which resulted from the scaffold use resembled a natural tendon and were abundant in tenocytes and collagen. Its breaking strength was about 83 percent of a normal tendon at 14 weeks [49]. However, along with being short living and terminally differentiated, the use of tenocytes still has one major problem, which is the harvesting of autologous tenocytes. Tendons are hypocellular tissues, and the harvest of autologous tenocytes can cause donor site morbidity [9].

As an alternative to tenocytes, other cell types are being studied to promote tissue regeneration. These include human dermal fibroblasts [50], adipose derived stem cells [51], bone marrow-derived stem cells [46, 52, 53] and human embryonic stem cells [54]. Mesenchymal stem cells are multipotent stem cells that have the ability to differentiate into several types of cell depending on the environment. Using growth factors, it is possible to control the differentiation of the cell. These cells may be obtained from many sources including adipose tissue, bone marrow, muscle and umbilical cord [55]. As for the growth factors, these can be added to the culture or secreted by stem cells. They are soluble secreted signalling polypeptides which instruct specific cellular responses in a biological environment. These factors are signalling molecules that stimulate cell proliferation, and differentiation. Besides growth factors, mitogens and morphogens are also signalling molecules which aid in this process and by regulating these molecules, it is possible to allow control over the regenerative process. PDGF (platelet-derived growth factor), FGF (fibroblast

growth factor), TGF (transforming growth factor) are some example of growth factors employed in tissue engineering [56].

As it was referred in Section 2.4 mechanical stimulation is vital to the recovery of the tissues after injury. Mechanical stimulation modulates cell behaviour. Cyclic strain in *in vitro* conditions, has great effects on tenocyte functions such as their metabolism and the increase of the mechanical properties of the resulting tissue [57, 58]. Various studies have also reported positive results on the mechanical stimulation of tissue engineering constructs [33, 59-61]

3.3 Fibrous structures

Scaffolds may be designed in different forms which include foams, sponges, hydrogels, meshes, fibres and more. The architecture of the scaffolds depends mainly on the properties of the material used and, on the purpose and function of the scaffold. For tissue engineering, fibrous scaffolds present some advantages when compared to other types of scaffolds. These structures are fabricated using fibres or yarns of synthetic or natural polymers. Fibrous scaffolds also allow 3D (three-dimensional) culture instead of 2D (two-dimensional). This supports a higher cell density than flat 2D surfaces. These scaffolds also present high porosity, isotropic structure and homogeneous fiber and consequently pore size [44].

Parallel fibres are the simplest fibrous structure. However, the lack of interaction between the fibres narrows its application [62]. Fibrous structures are usually used in woven, nonwoven, knitted, braided and electrospun. Each textile type has its physical and mechanical properties and the type of textile used will depend on the required properties of the application. Woven structures exhibit the highest strength value and are suitable for long term applications. Knitted structures, as opposed to woven, are anisotropic. The yarn changes directions continuously through the fabric. Also, the yarn density is lower than in woven textiles which increases structure porosity. They exhibit lower mechanical strength than woven structures, but the possibility of inserting holes in the structure enhances surface area and permeability which promotes tissue ingrowth. Braided structures consist in three or more yarns intertwined over each other. These structures have the highest axial strength compared to other textiles. Therefore, they are excellent for high in-plane mechanical strength. Due to their structure they can withstand high loads and

provide extension. Porosity and mechanical properties can be tuned by varying structural factors such as number of yarns, yarn angle relative to the vertical direction. Nonwoven structures were introduced in the 1990s and were used mostly under the name Ethisorb™. Nonwoven structures are more random than the previous. Due to this randomness, sometimes is necessary to strengthen the structure by bonding the fibres in the web [63]. More organized structures such as woven, braided and knitted scaffolds may provide an oriented growth for cells, which has great impact on cell behaviour [64, 65]. In studies found for Achilles tendon scaffolds, knitted structures were used the most. [62, 66-68]. This is mainly due to the high porosity, and consequently, high ability to support tissue ingrowth exhibited by knitted structures when compared to braided structures [62, 66]

Eichhorn et al. demonstrated the relationship between the fibre diameter and pore size [69]. Nanofibrous scaffolds have many advantages compared do microfibrous scaffolds, such as more surface area to volume ratio and better mimicking of the ECM structure. However, the small diameter of these fibres reduces pore size and interconnectivity, thus provides a 2D environment for cell growth instead of 3D. This limits the cell attachment greatly, as cells cannot infiltrate the scaffold which limits cell proliferation [70]. Cells behave much differently in 2D and 3D matrixes. Pore size and high interconnectivity are very important for cell infiltration, cell interaction and nutrient and waste transport [71]. As an attempt to solve this issue, a scaffold with hybrid fibre size composed by nano- and microfibres was investigated [44]. This enables to get the cell attachment provided by the nanofibers with the structural support of the microfibres and bigger pores. Tuzlakoglu et al. studied these hybrid structures using type I collagen nanofibers and starch-based microfibres. The use of this combined structure increases the metabolic activity of the cells and cell growth [72]. However, limited cell migration is observed due to the nanofibers in these scaffolds [73].

Other methods are available to utilize the qualities of nanofibers without having the problem of having small pores. For example, Lee et al. suggested the use of micro-voids in nanofibrous structures to improve cell migration [74]. In another study, Thorvaldsson et al. used electrospun nanofibers to coat single microfibres. Cellular infiltration and proliferation were observed along the coated microfibres of the scaffold, and which also maintained their surface and structural properties [75].

Commercial synthetic fibrous scaffolds used in ligament and tendon tissue engineering include Gore-Tex®, Lars-Ligament®, Leeds-Keio®, and SportMesh™. The first four are non-absorbable scaffolds with the last being absorbable. All are approved by the FDA (Food and drug administration), except for the LARS ligament [63, 76, 77]. Gore-Tex® ligament is made of continuous multifilament yarns of tightly braided microporous PTFE (polytetrafluoroethylene). Its tensile strength is twice the human ACL and has higher stiffness. With this said, it was a very promising material. It was used worldwide between 1982 and 1990. Sterile synovitis, effusion and rupture were observed. Infection was also reported in 2-3% of the cases. Loosening of initially well-tensioned grafts was also reported, and localized inflammation originated by microbreakage and particle debris. Poor healing of the ligament was also observed. Initially, the implant presented good stability, which was deteriorated over time. It was removed of the market by the manufacturer by bad results (44% failure rate at 5 years) [63].

LARS ligament is a second-generation, non-absorbable synthetic ligament composed by PET (polyethylene terephthalate) fibres. It has been approved by health authorities in Europe and Canada but not by the FDA for a wide range of applications such as ACL reconstruction, Achilles tendon repair and acromioclavicular repairs. It exhibited good results in the repair of collateral ligaments [78], posterior cruciate ligament [79] and anterior cruciate ligaments [80]. It exhibits good mechanical strength and biocompatibility to long term implantation [77].

The Leeds-Keio graft is an artificial ligament, formed by PET fibres, especially designed to ACL reconstruction, hence its stiffness, 200N/mm, similar to the ACL [81]. Adverse results were reported regarding the use of this graft such as rerupture, synovitis and laxity were reported [82-84]. However, positive results also were reported [85, 86]. Leeds-Keio was also used for repairs of rotator cuff tear [87], Achilles tendon rupture [88], and ankle lateral ligament repair [89].

Artelon® and SportMesh™ are made of biodegradable polyurethane urea (PUU), and it has been cleared in Europe and by the FDA for reinforcement of soft tissues such as rotator cuff, Achilles tendon, patellar, biceps and quadriceps. The Artelon® fibre is a slow degrading, biodegradable, with good mechanical properties which also

promotes cell ingrowth [90-92]. After 3 years of surgery, no adverse effects were reported and the results using Artelon® were better than in the control group [93].

Table 2 – Commercially used synthetic fibrous grafts

Product	Material	Absorbable/Non-absorbable	Structure	Function	Company	Ref.
Gore-Tex®	PTFE	Non-absorbable	Braided	ACL	WL Gore and Associates, USA	[8, 77]
LARS-Ligament®	PET	Non-absorbable	Parallel longitudinal fibres (intraarticular portion)	ACL	Ligament Augmentation and Reconstruction System, Dijon, France	[8, 77]
Leeds-Keio®	PET	Non-absorbable	Woven	ACL	Xiros plc, Neoligaments, Leeds, UK Yufu Itonaga Co. Ltd, Tokyo, Japan	[8, 77]
SportMesh™ /Artelon®	PUU	Absorbable	Woven	Rotator cuff, Achilles Tendon	Artimplant	[63]

4. Biomaterials

4.1 Biodegradable polymers

Natural polymers such as collagen have been used in biomedical applications for many years, but the use of synthetic biodegradable polymers is relatively new, beginning in the 1960s. Since then, its use is growing greatly, being nowadays a field of much research. The rise of these materials is linked with their use in tissue engineering, regenerative medicine, gene therapy and bionanotechnology, all of which require biodegradable platform materials to build on. The biodegradable polymers have had tremendous success over the years, but great challenges remain in the design of biomaterials [94].

In designing biodegradable biomaterials, many important characteristics must be considered. They must not evoke a sustained inflammatory response, possess a degradation time coincident with their function, have the appropriate mechanical properties for the application, the products of the degradation must be non-toxic and need to be available to be readily resorbed or excreted and present the appropriate permeability and processability. These characteristics are a result of

many properties of the degradable polymeric biomaterials such as material chemistry, molecular weight, hydrophobicity, water adsorption, degradation and erosion mechanism [95].

4.2 Degradation of Biodegradable polymers

The difference between biodegradable polymers and regular polymers is their degradation, which is a valuable characteristic in biomedical applications. This means, it is important to study the degradation of these materials and its mechanisms. The biodegradability of a polymer mainly depends on its backbone structure. They depend on repetitive unit, composition, sequence length, molecular geometry, molecular weight, morphology, hydrophilicity, surface area and additives [96]. Biodegradable polymers can be degraded hydrolytically, enzymatically or both. Normally, natural polymers undergo mostly enzymatic degradation. However, the rate of *in vivo* degradation depends varies largely on the implantation site. Synthetic biodegradable polymers, on the other hand, degrade mostly by hydrolysis. These are preferred to be used in implants due to minimal site-to-site and patient-to-patient variations, when compared to enzymatically degradable polymers. Hydrolytically degradable polymers are polymers that have less stable chemical bonds in their backbone. This means their functional groups are susceptible to hydrolysis, and these can be: esters, ortho esters, anhydrides, carbonates, amides, urethanes and more [96, 97].

Usually, there are two main possibilities to synthetize hydrolytically degradable polymers, it can be through step polymerization or addition polymerization, including ROP (Ring opening polymerization). Step polymerization is used to produce polyanhydrides, poly(ortho esters) and polyurethanes. ROP is used to develop hydrolytically sensitive polymers as poly(α-esters) and polyphosphazenes. Poly(α-ester) can also be synthetized through bacterial bioprocesses [94].

4.2.1 Polymeric degradation by hydrolysis

Hydrolytically degradable polymers are polymers that have unstable chemical bonds that can break through the interaction with water. When the bond is broken, it yields two species with one gaining a hydrogen ion (H^+) and the other gaining a hydroxyl group (HO^-). Ester bonds are an example of these hydrolytically unstable bonds. These reactions depend on pH can be catalysed by acids, bases and enzymes [95].

This chain scission process reduces chain entanglement rapidly, and subsequently, reduces strength [98].

After immersion of the polymer in the aqueous medium, the first event that occurs is water uptake, and it continues until saturation. The maximum water uptake of a polymer depends on its hydrophilicity, crystallinity, temperature, pH and flow of the media. This leads to swelling, or, increase in volume. At this point, water molecules are in the polymer structure and start triggering the degradation of the polymer by cleavage of the polymer chains [99].

There are two characteristics that are very important for the use of these materials in biomedical applications: degradation rate and the erosion mechanism. The degradation rate can vary considerably, from very unstable polymers (polyphosphazenes) to stable polymers (polyamides). An extremely important feature of these polymers is the ability to modulate the degradation rate of the material through the chemistry, conveying a significant flexibility on the properties of the material [95].

The degradation of a polymer depends of factors such as water diffusion, solubility of the monomers, geometry, dimension of the implant, molecular weight, glass transition temperature (T_g) and hydrophobicity. Hydrophobicity is intimately connected with the ability of the polymer to absorb water. Hydrophilic polymers absorb substantially more water than hydrophobic polymers. The morphology of the material also influences the degradation rate, with greater crystallinity implicating less hydrolysis reaction and porosity being directly proportional to hydrolysis [95, 98]. Among the characteristics of the material, biodegradation also depends on extrinsic factors. These factors include: pH of the degradation media, type of electrolytes present in the degradation media, the external stress/strain applied on the material, temperature of the degradation media, free radicals, enzymes, bacteria, lipids, synovial fluid and if the material was exposed to γ-radiation [100].

Determining the type of erosion that takes place in the degradation of a polymer is essential as it is directly related to its application. It can be through surface erosion or bulk erosion. Surface erosion happens when the degradation rate at the interface water-polymer is much higher than the rate of the water diffusion to the bulk of the material. This results on a degradation that takes place mostly on the surface, with

the core remaining intact (retaining average molecular weight and mechanical properties). The load bearing capability decreases steadily until the thickness of the polymer reaches the critical thickness. When this happens, the erosion process shifts from surface to bulk erosion, where the time to failure is controlled by the auto-acceleration of the hydrolysis. In this phase, the M_w (weight-average molecular weight) reaches its critical value, where the polymer depolymerises into water soluble products [98]. Polymers which degrade through surface erosion are particularly indicated for drug delivery applications [101]. Bulk erosion is characterized by the opposite situation, where the water diffusion rate is greater than the degradation rate on the surface, resulting on degradation throughout the material. PGA and PLA are two examples of polymers which undergo bulk erosion. In this erosion process, a decrease in molecular weight is seen before mass loss is observed [98]. The representation for the bulk and surface erosion processes and their influence on properties is shown in Figure 7.

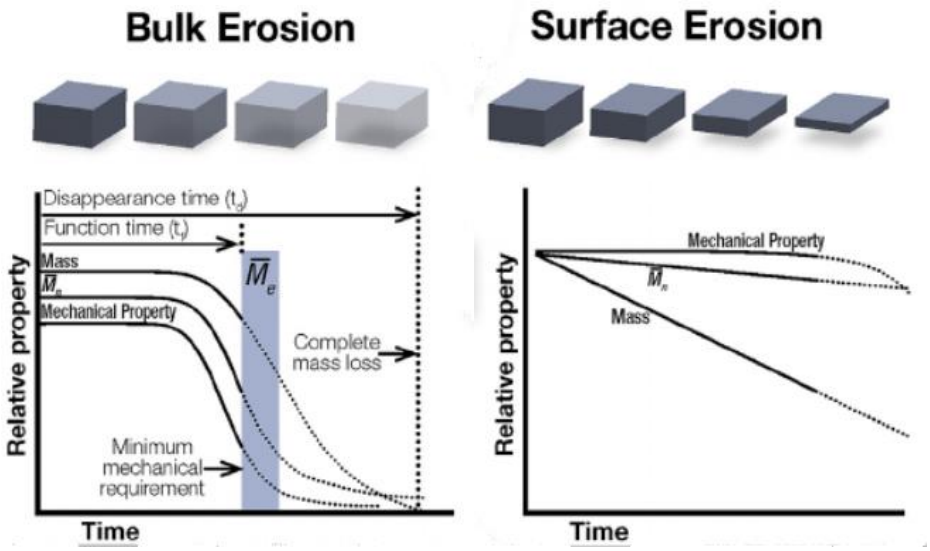

Figure 7 - Surface and bulk degradation and their effects (adapted from [98])

4.2.2 Enzymatic degradation

Exposing polymeric biomaterials to bodily fluids and tissues can result in a degradation process of the polymer due to enzymatic activity. When the body reacts, and starts an inflammatory response to the material, the cells which are responsible of defending the organism, mainly leukocytes and macrophages, release extremely reactive specimens such as superoxides (O^{2-}), hydrogen peroxide (H_2O_2), nitric oxide (NO), and hypochlorous acid (HClO). The oxidative effect of these specimens can contribute to the cleaving of polymer chains and their degradation [102]. Lee et al.

studied the oxidative effect of superoxides in absorbable sutures, and it was concluded that these specimens accelerate the process of degradation of the sutures and affect mechanical and thermal properties along with surface morphology. The amounts of tensile breaking force loss during the first 24h ranged from 3% to 80% depending on the absorbable suture [100].

Hydrolysis can also be catalysed by enzymes such as proteases, esterases, lipases glycosidases and phosphatases. These enzymes are responsible for many reactions that happen in the human body [103]. The effect of lipases in the degradation of PCL was studied [104]. It showed that PCL (polycaprolactone) is sensible to the presence of pseudomonas lipase. However, the presence of PP lipase (porcine pancreatic) and candida cylindracea lipase did not have the same effect. This fact can help explain the fact of why the degradation rates *in vivo* are higher than in *in vitro* tests.

In semi-crystalline polymers, when the degradation takes place due to enzymatic activity and hydrolysis, the process occurs in two phases. Firstly, water diffuses into the polymer and attacks the chemical bonds, preferably in the amorphous region, breaking longer polymeric chains into short chains, until there are only fragments soluble in water. As this happens first in the amorphous region, there is loss of molecular weight without decreasing mechanical properties as it is the crystalline region that holds the matrix. After, the degradation begins heavily on the crystalline region which result on the loss of mechanical properties. On the second phase, the enzymatic attack to the fragments generated in the process takes place. This metabolization results on fast loss of polymer mass [102].

4.3 Aliphatic polyesters

Aliphatic polyesters (or Poly(α-ester)s) are thermoplastic polymers which are greatly used as biomaterials due to their hydrolytically labile aliphatic ester bonds in their backbone and the products of the hydrolysis reaction are naturally metabolized by the human body. Theoretically, all polyesters are degradable as esterification (reaction between, usually, an acid and an alcohol, to from ester as the reaction product) is a chemically reversible process, but only poly(α-ester)s with short aliphatic chains between ester bonds can degrade over the time frame required to most biomedical applications. Polyesters can be synthetized from a variety of

monomers via ring opening polymerization and condensation polymerization routes depending on the monomeric routes [105].

4.3.1 Polylactic acid (PLA)

Lactide is a chiral molecule and can exist in two forms: D-Lactide, L-lactide. These can form PDLA (Poly-D-lactic acid) and PLLA respectively. The polymerization of these monomers will result in the formation of semicrystalline polymers. The polymerization of D, L-lactide and mesolactide will result in amorphous polymers. Among these monomers, L-lactide is the naturally obtaining isomer. It is a semi-crystalline polymer with around 37% crystallinity, with this being a result of the molecular weight and processing parameters. The glass transition temperature is between 60-65ºC and the melting temperature is approximately of 175ºC. Compared to PGA, PLLA is a slow-degrading polymer, with lower tensile strength and good extension. Due to these properties, PLLA has been largely investigated as a scaffolding material for ligament replacement [94]. It is approved by the FDA for use in the human body [106]. Polylactides undergo hydrolytic degradation via bulk erosion, by the scission of the ester backbone. The degradation of the polymer results in lactic acid, a normal human metabolic by-product, which is broken down into water and carbon dioxide. Being more hydrophobic than PGA, this polymers degradation is much lower. However, the degradation depends on crystallinity and porosity of the matrix. It has been reported that high molecular weight PLLA can take more than 5 years for total resorption *in vivo* [107]. PLA also undergoes enzymatic degradation when in low crystallinity polymers. Proteinase K degrades preferably L-L bonds, followed by D-L bonds and finally D-D bonds [108, 109]. Due to its semi-crystallinity PLLA is preferred over PDLLA (Poly-D, L-lactic acid) in applications where high tensile strength and toughness are required. It is known that the polymer loses its mechanical properties due to hydrolysis after approximately 6 months, but no significantly changes in the mass occurs for a long time. PLLA is used in FixSorb®, as a bone fixator [110] and in tissue engineering for bone [111], vascular [112], cartilage [113] and tendon [114] applications. PDLLA is an amorphous polymer due to random distribution of L- and D- lactide units and has a glass transition temperature of 55-60ºC. Since it is an amorphous material, it shows lower tensile strength than PLLA. It loses its mechanical properties after 1-2 months due to hydrolysis and mass loss happens within 12-16 months. Since it degrades faster than

PLLA and has an amorphous structure which allows a homogeneous distribution of the active species it is a better candidate to drug delivery systems. Its degradation rate can vary according to the percentage of D- and L- in the polymer structure [94, 96, 97].

4.3.2. Poly(lactide-co-glycolide) (PLGA)

The result of the copolymerization of PLA (both the L- and the DL-lactides) and PGA is PLGA. This is the most investigated copolymer for biomedical applications such as sutures, drug delivery systems and scaffolds for tissue engineering. It has great availability and processability. Since PLA and PGA have different properties, it is possible to adjust the ratios of both polymers and obtain a large range of properties. Poly(lactide-co-glycolide) with 25-75% ratio, forms an amorphous polymer, very hydrolytically unstable compared to the homopolymers. At 50/50 ratio, the copolymer is even more unstable, since the degradation resistance is higher at both ends of the copolymer composition range. At this ratio, the copolymer degrades at approximately 1-2 months. [94, 115]. The copolymer undergoes bulk erosion through hydrolysis of the ester bonds and the degradation rate depends on some parameters such as LA/GA ratio, molecular weight and the shape and structure of the matrix. An advantage of this polymer is the fact that it is FDA approved for use in humans, and its good processability that enables the production of a variety of structures and forms and control the degradation rates of the polymer, hence being the most investigated copolymer for biomedical applications. PLGA also shows good cell adhesion and proliferation, which is essential for tissue engineering applications. Many studies have been made using micro- and nano- fabrication techniques to create 3D scaffolds based on PLGA [94, 95]. Regarding the enzymatic degradation of PLGA, enzymes may enhance the degradation of this polymer but hydrolysis is still the main process for the degradation of PLGA [116].

PLGA is used widely in biomedical applications including sutures such as Vicryl®, Vicryl Rapide®, Panacryl®, PolySorb® and PuraSorb®. It has also been used in drug delivery applications [95]. In tissue engineering applications, PLGA has been used to produce scaffolds for tendons and ligaments [67, 117], vascular [118], cartilage [119] and cardiac [120] applications.

4.3.3. Polycaprolactone (PCL)

Polycaprolactone is a hydrophobic, semicrystalline polymer, obtained primarily by ROP of the monomer ε-caprolactone. It has good processability and solubility and exceptional blend-compatibility. It has a low melting temperature of 59-64ºC and a glass transition temperature of -60ºC. Its crystallinity tends to decrease with the increase of molecular weight. PCL undergoes surface hydrolytic degradation by the cleavage of the polymer backbone. It is a hydrophobic polymer with a very slow degradation rate (can reach up to 3-4 years), therefore it was originally used in drug delivery systems that are active for 1 year or more. It is used on Capronor®, which is a commercial contraceptive PCL product that delivers the active substance for over a year. It is FDA approved for some medical devices and for drug delivery systems [95, 121]. As for the enzymatic degradation of this polymer, it has been shown that PCL degrades rapidly in the presence of pseudomonas lipase [104]. When compared to other biodegradable polymers, this polymer has superior rheological and viscoelastic properties, high permeability to small drug molecules, maintenance of a neutral pH environment during degradation, and its slow erosion kinetics compared to PLA and PGA, characteristics which are important to biomedical use. As a result of these adequate properties for tissue engineering applications, PCL is widely used to form copolymers for scaffolds. It has been investigated in many fields of tissue engineering such as scaffold for tendons and ligaments [122]

4.3.4. Polytetrafluoroethylene – (PTFE)

While not being an aliphatic polyester, PTFE was investigated due to its use in this work. Polytetrafluoroethylene is a semi-crystalline fluoropolymer, classified as a thermoplastic. It was discovered at the DuPont industry and is mostly known for its commercial name Teflon®. This polymer has some characteristic properties such as high mechanical strength, high chemical inertness, hydrophobicity and high thermal conductivity in composite form. It is a high thermal resistance and high operating temperature polymer with a melting temperature between 325ºC and 335ºC. PTFE is used in several fields including automotive industries, food processing, petrochemical, electrical, chemical and biomedical applications. [123] In the field of biomedicine, the application of PTFE includes biliary stents [124], vascular grafts [125], tissue engineering [126].

In the 1980s, PTFE, in the form of expanded PTFE began to be used as a ligament prosthesis with the name Gore-Tex®, especially in ACL repair. It was approved by the FDA for use in patients with previously failed autologous ACL reconstructions. It demonstrated very high tensile strength and stiffness. Its goal was to replace the ACL permanently and promote fixation and early load-bearing capacity [8]. After good preliminary results [127, 128], the ligament prothesis started to show complications such as, effusion and pain [129] presence of wear debris [130], and loosening [131]. In 1993, it was withdrawn from the market and abandoned in knee instability surgery [8].

4.5.5. Polydioxanone – (PDS)

Polydioxanone, known as PDS, PDO, or poly(p-dioxanone), is a colourless, crystalline, bioabsorbable polymer mostly known by its clinical use as a monofilament suture. This polymer is poly(ester-esther) and was introduced in the market by Ethicon Inc. in 1981. It is synthetized by ring-opening polymerization through the monomer paradioxanone, or p-dioxanone. This polymer presents a crystalline fraction of 55% and Tg is between 0ºC and -10ºC. As a suture, its shows good flexibility, good strength retention, slow absorption rates and low inflammatory response [132, 133]. Its shape memory characteristic is one important disadvantage for its use as a suture, as it can make knot retention difficult. PDS is approved by the FDA to be used as a suture material [134].

Polydioxanone degrades through hydrolysis in two stages and undergoes a “cleavage-induced crystallization process”. First the amorphous regions suffer degradation, which leads to an increase in crystalline content, followed by the degradation of the crystalline regions. [133] When degraded in an enzymatic medium such as bile and pancreatic juice mixture, this polymer showed minimal tensile strength changes [135].

Besides suturing, PDS is also present in applications including orthopaedics [136], cardiovascular [137, 138] and bone tissue engineering [139]. Oryan et al. utilized polydioxanone as a sheath in a collagen-PDS based tissue engineered graft employed to repair a large defect on the Achilles tendon in rabbits. It was concluded that the artificial tendon accelerated tendon healing and resulted in a new tendon which was biomechanically, biochemically and morphologically tendinous in nature. The

tendons regenerated by this artificial tendon also demonstrated better mechanical properties than the controls. [140]

5. Methodology

In this study, the design of scaffolds and simulation of their mechanical behaviour for the regeneration of the Achilles tendon were made based on a simplified approach. According to J. Banks [141], a simulation study is composed by a set of steps. It begins with a statement of the problem followed by setting the goals of the simulation and overall project plan, model conceptualization, data collection.

With this in mind, the first point was to define the problem. The field of scaffolding for ligaments and tendons, while it has been widely studied nowadays, still lacks information regarding the ideal composition and the outcomes of the use of synthetic biodegradable scaffolds for tendons and ligaments in humans. Especially on the mechanical behaviour of the scaffold with degradation time and the properties of the resulting tissue. The goal of this work was to design a scaffold and simulate, based on a simplified approach, the mechanical behaviour of the scaffold and the regenerating Achilles tendon tissue during degradation/regeneration. The function of the scaffold is that it should provide mechanical support to the tissue to prevent its rupture. This support given by the scaffold is crucial in the earlier stages of regeneration, when the regenerating tissue does not yet possess the mechanical properties which allow normal load bearing without tissue failure.

The scaffolds were designed using biocompatible polymers which were previously used in biomedical applications. Data regarding the mechanical properties of the materials during degradation were obtained from the literature. Regression models were employed to obtain the mathematical expressions that represent the evolution of those properties with degradation time. The same was made to obtain the expressions that translate the growth of the tissue and its mechanical properties. Information regarding simulation parameters, scaffold sizing, characteristics of a normal Achilles tendon and characteristics of an injured Achilles tendon were also obtained from the literature. Two different scaffolds were designed, one fully degradable and another semi-degradable, where the fully degradable scaffold was composed by biodegradable polymers only and the semi-degradable was composed by biodegradable polymers and one non-degradable polymer. The rationale behind

the utilization of the semi-degradable scaffold is that, since an Achilles tendon presents lower mechanical properties after healing from a total rupture than a healthy Achilles tendon, the scaffold would possess a non-degradable portion which would provide reinforcement to the weaker tissue even after the healing process is concluded. This would result in a scaffold that could degrade partially and promote tissue regeneration but also provide permanent mechanical support to the injured tendon. The effectiveness of the semi-degradable scaffolds for tissue regeneration could be explored further.

As referred previously, the design of scaffolds is very complex. They must present specific characteristics to ensure its success, such as high porosity to promote cell attachment and proliferation, not producing debris which would impair the environment *in situ* and exhibiting a stiffness within a certain range. However, in this work, the focus was mainly on the mechanical factors. Biological, chemical and physiological aspects were disregarded in this model. While seeking to fulfil some of the requirements imposed by these aspects in an earlier stage such as using biocompatible materials exclusively and designing a scaffold with an initial stiffness close to a normal Achilles tendon, other were not considered. For example, PTFE which has shown some problems in the field of ligament reconstruction, was used in this investigation due to its use in the human body as the FDA approved Gore-Tex® artificial ligament.

The simulation was implemented in a spreadsheet using an algorithmic procedure described in Section 5.6. It allowed the input of the expressions that give the evolution of the mechanical properties of the elements with time and to study how the loads are distributed through the elements at each time step.

This work was made to approximate *in vivo* conditions as close as it was possible but as this is a simplified model, many aspects do not correspond to the real, *in vivo* conditions. The limitations of this model are discussed further in this work.

5.1 Data collection

For the purpose of this investigation, data regarding the evolution of mechanical properties during degradation of some polymers, and the evolution of the mechanical properties of the Achilles tendon while regenerating from a total rupture were collected. All data was collected from the literature for further use in the simulation.

In this study, six articles are considered to represent the properties of the components (PLA-PCL, PLGA, PDS, PTFE and Achilles tendon tissue). One study to represent the mechanical properties of each polymeric material and two to represent the Achilles tendon tissue. From the two studies used to represent the natural tissue, one study was used to represent the properties of a healthy and a previously ruptured Achilles tendon, and another study to represent the evolution of the mechanical properties during healing of a total Achilles tendon rupture.

5.2 Data selection

The selection criteria were:

Materials:

- Materials that could degrade within the human body without promoting any prejudicial reactions from the host (Not applied to the non-degradable material);
- Materials with mechanical properties that enable the production of a scaffold for the Achilles tendon;
- Biocompatible materials;
- Materials that are already approved for use in the human body by the FDA.

Material data source:

- Studies that reported the degradation of mechanical properties of the selected material;
- Studies in which the degradation tests were made *in vitro* and had the goal of approximating itself to *in vivo* conditions (such as degradation medium, temperature);
- Studies on materials that exhibited an evolution of mechanical properties suitable for the application, such as Young's Modulus and tensile strength appropriate to the Achilles tendon tissue;
- Studies that investigated the materials under the form of suture or scaffold for comparison purposes.

Achilles tendon properties during regeneration data source:

- Studies that reported the cross-section area and the Young's Modulus during the regeneration of the tissue after rupture;
- Studies in which the regeneration of the tendon happens after an Achilles tendon rupture;
- Studies in which the Achilles tendon rupture is repaired by surgical suturing intervention;
- Studies performed in humans;
- Studies where the measurements were made *in vivo*.

Injured and the uninjured Achilles tendon data source:

- Studies in which cross-section area, tensile strength, Young's Modulus and tendon length were measured;
- Studies in which the injured tendon suffered an Achilles tendon rupture;
- Studies in which the injured tendon was repaired by surgical intervention for coherence purposes.

In the articles where the same material was presented in different forms e.g. fibres with different diameters, the option which would present more appropriate characteristics (such as Young's Modulus and tensile strength) to reach our desired scaffold properties was chosen.

5.3 Data presentation

As reported before, the materials chosen to compose the scaffolds were PLGA, PLA-PCL, PDS and PTFE. In table 3, information regarding the studies of the materials selected for this investigation is shown.

In this section, information about each considered research is presented. In ideal comparison conditions, all the studies considered should have utilized the same material form (fibres), but no suitable data sources investigating the degradation of mechanical properties in PLGA in the form of fibres were found. Therefore, a research studying PLGA in the form of a knitted fibrous scaffold was considered.

Table 3 - Data regarding the studies of the materials chosen for this investigation

	PLGA	PLA-PCL	PDS	PTFE
Material composition	10% PLA 90%PGA	90%PLA 10%PCL	100% PDS	100% PTFE
Form	Scaffold	Fiber	Fiber	Fiber
Fiber diameter (mm)	0.225	0.4	0.15	0.02
Processing	-	Melt-spun	-	Melt-spun
Molecular Weight (M_n)	-	28000	-	121000
Degradation medium	Dulbecco's modified Eagle Medium	PBS	PBS	-

- **PLGA**

For PLGA, the article chosen was from Vaquette et al. studying the knitted scaffold for tissue engineering [52].

In their research, Vicryl suture 4-0 (poly (L-lactic-co-glycolic acid) (10/90) was used to fabricate a knitted scaffold, 6 stiches wide and 15 rows long with an internal stich diameter of 1mm. The average diameter of the fibres was of 225μm. The degradation took place in 15 ml tube containing 5ml of Dulbecco's modified Eagle's solution at 37ºC. The degradation medium was changed every 7 days. The samples were tested at 0, 7, 21, 28, 35, 42, 49 days of degradation.

Several characteristics were studied, such as, morphology, mechanical properties, degradation, inherent viscosity, pH and weight differences were investigated. For the mechanical tests, five samples were tested for each degradation stage. Biological evaluation was done, with the fabrication of a composite scaffold with cellularized alginate gel encapsulating the PLGA scaffold. For *in vivo* testing the scaffold was coated with alginate gel and fibroblasts in order to promote tissue growth. The data utilized in this work is regarding the scaffold without cellularized alginate gel encapsulation.

The tensile tests showed an initial tensile strength of 164MPa, and a Young's Modulus of 765MPa. The degradation of the scaffolds lasted 49 days, but after 42 days the scaffolds were too brittle to perform tensile tests. The Young's Modulus (Eq. 1) and the tensile strength (Eq. 2) were modelled using exponential functions.

$$E_{PLGA}(t) = 251{,}66e^{-0{,}003t} \quad (1)$$

$$\sigma_{r\text{-}PLGA}(t) = 1096{,}6e^{-0{,}002t} \quad (2)$$

- **Polylactic acid/Polycaprolactone blend – PLA-PCL**

For the PLA-PCL fibres, the data was withdrawn from Vieira's work [142].

The degradation of the mechanical properties of PLA-PCL fibres were studied in PBS (phosphate buffer saline), water and NaCl solution for 16 weeks at 37ºC. The fibres were inserted in test tubes and submitted to different degradations stages. The samples were weighed before and after degradation and GPC (gel permeation chromatography), monotonic tensile tests, dynamic mechanical analysis were performed, along with biocompatibility, thermal and chemical characterization. For this investigation, the data regarding the degradation of PLA-PCL fibres with a diameter of 400µm degraded in PBS was used. The composition of the fibres of was 90%PLA and 10% PCL, with a Tg of 56ºC and Tm (melting temperature) of 157ºC.

In his study, the author modelled the degradation of the fibres and presents the mathematical expression for the loss of tensile strength during the degradation of the fibres, shown in Eq. 3, therefore it was not necessary to calculate the model for the degradation of tensile strength for this material.

$$\sigma_{r-PLA-PCL} = \sigma_0 e^{-kt} \quad (3)$$

In this equation, σ_0 is the initial tensile strength of the fibre, *k* a constant which depends on the degradation media and *t* stands for time.

As for the evolution of the Young's Modulus of PLA-PCL fibres (Eq. 4), was obtained through modelling using the data gathered, using a linear function.

$$E_{PLA\text{-}PCL}(t) = 0{,}7054t + 1197 \quad (4)$$

- **Polydioxanone - PDS**

For PDS, a study from Zilberman et al. regarding the degradation of bioresorbable sutures was used [143].

In this research, the authors focused on the mechanical properties during *in vitro* degradation of some bioresorbable fibres and stents, using polymers such as PLLA, PGACL (poly (glycolic acid-co-ε-caprolactone)) and PDS. For our work, only PDS fibres

were considered. PDS was used in the form of monofilament fibres obtained from Ethicon, Inc. with a diameter of 0.15mm.

For the characterization of the fibre samples, fibres were weighed to determine weight retention, tensile testing and observation through SEM (scanning electron microscopy) were performed. The mechanical properties were studied during *in vitro* degradation over six weeks at 37ºC in PBS solution. Samples were tested every week, and five samples were tested for each point.

In their investigation, PDS showed a moderate tensile strength and Young's Modulus and relatively high ductility when compared to the other tested fibres. The polymer presented an initial elastic modulus of 365MPa and a tensile strength of 612MPa. After six weeks of degradation, PDS lost 2%wt and preserved its mechanical properties partially. The Young's Modulus (Eq. 5) and the tensile strength (Eq. 6) of PDS were modelled using linear functions.

$$E_{PDS}(t) = -0{,}0418t + 367{,}3 \quad (5)$$

$$\sigma_{r\text{-}PDS}(t) = -0{,}2198t + 613{,}01 \quad (6)$$

- **Polytetrafluoroethylene – PTFE**

To represent the properties of PTFE, a study from Goessi et al. regarding the characteristics of different grades of PTFE was chosen [144].

In their study, they reported a set of PTFE grades in the form of melt-spun monofilaments. These fibres were spun at 380ºC and varied in weight-average molecular weight, and consequently, in mechanical properties. The fibre diameter was of 20µm. The characterisation of the fibres included DSC (differential scanning calorimetry), tensile testing and Wide-angle X-ray analysis.

The fibre grade elected to represent the properties of PTFE used in this study is IX. This grade was chosen due to it high Young's Modulus. This grade exhibits a weight-average molecular weight of 202kg/mol, a melting temperature of 320ºC. As for the mechanical properties, they are shown in table 4.

Table 4 - Mechanical properties of PTFE

Property	**Value**
Tensile Strength (MPa)	176
Young's Modulus (MPa)	1656

This material was chosen as the non-degradable polymer to be used in the design of the semi-degradable scaffold due its previous utilization in biomedical applications as Gore-Tex® artificial ligament in knee surgery. As said previously, it is known that this artificial ligament led to many problems such as wear debris and loosening, however, these aspects are neglected in this simplified model.

- **Natural Achilles Tendon Tissue**

To represent the mechanical properties of the uninjured Achilles tendon and the mechanical properties of the injured Achilles tendon after healing, the article chosen was from Geremia et al. [145].

In their study, an evaluation of early mobilization and traditional immobilization after an acute rupture of the Achilles tendon was made, by comparing the stress-strain and force-elongation relationships of the injured tendon to those of the uninjured tendon. A group of males with previous Achilles tendon rupture (n=18) and a group of healthy male control participated (n=9). Half of the Achilles tendon rupture group have received early immobilization while the other half received traditional immobilization with a plaster cast.

To determine the cross-sectional area, tendon resting length and tendon elongation as a function of torque during the maximal voluntary plantar flexion, ultrasound was used. Achilles tendon force-elongation and stress-strain relationships were determined from these data. In table 5, data regarding an uninjured Achilles tendon and a tendon that suffered a total rupture and had a regeneration time of 2 years are presented. The values used for the injured tendon are regarding tendons which underwent short-term physiotherapy. This choice was based on the studies which report that mechanical stimulation enhances tissue regeneration in scaffolds [59-61] and studies that report positive results regarding early mobilization after an Achilles tendon rupture [28].

The value of breaking tensile strength of the Achilles tendon was obtained from [146] for a displacement speed of 10mm/s.

*Table 5 - Properties and characteristics of healthy and injured tendons (*value of tensile strength was obtained from [161])*

	Young's Modulus (MPa)	Maximum voluntary stress (MPa)	Stiffness (N/mm)	Force (N)	Elongation (mm)	Strain (%)	Cross-section area (mm^2)	Tendon Length (mm)	Tensile Strength (MPa)
Uninjured Tendon	848	54	228	3294	16	6.86	62	237	86*
Injured Tendon	369	23	166	2556	15	6.45	128	244	-

- **Mechanical Properties of the regenerating Achilles tendon**

To represent the properties of the regenerating Achilles tendon the investigation from Schepull et al. was used [147].

In this study, the Achilles tendon repair was studied in ten patients with total Achilles tendon rupture with RSA (Roentgen stereophotogrammetric analysis). Tantalum beads were implanted in surgery. Evaluations were made at 6, 12, 18 weeks and 1 year. RSA was performed with two different mechanical loadings and the strain induced by increasing loading was measured. The transverse area was determined by ultrasound.

The data regarding the evolution of the Young's Modulus and the cross-section area of the Achilles tendon during regeneration are shown in Figure 8 and 9, respectively.

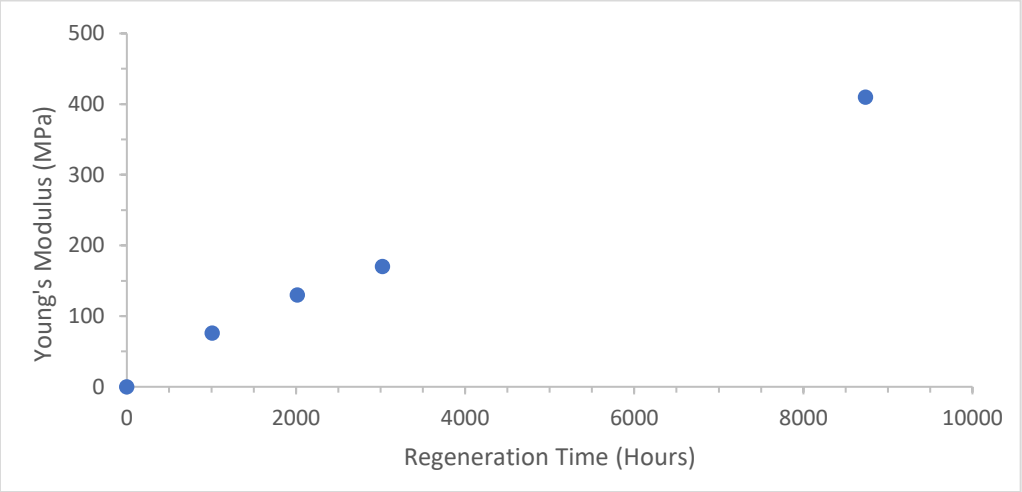

Figure 8 - Values of Young's Modulus during healing from an Achilles tendon rupture obtained from [144]

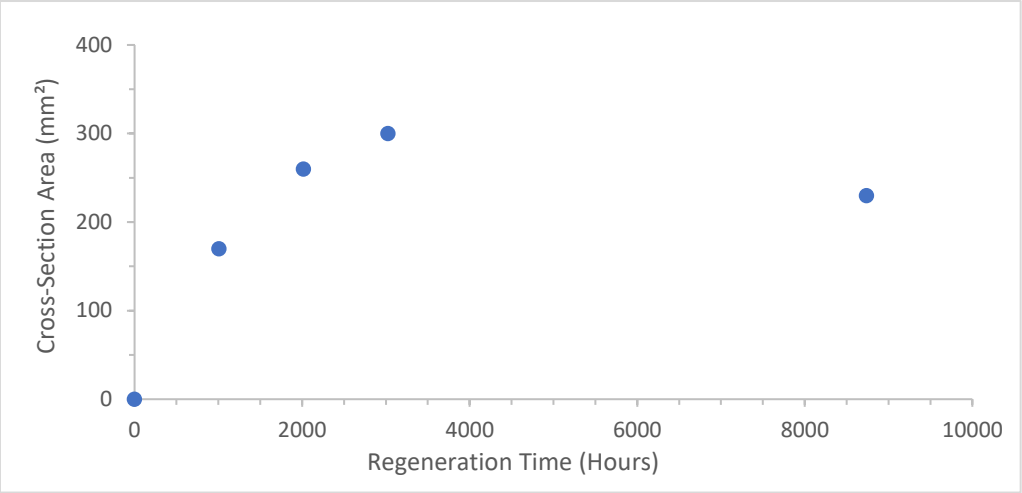

Figure 9 - Values of cross-section area during healing from an Achilles tendon rupture obtained from [144]

5.4 Modelling the evolution of properties of the materials and the regenerating Achilles tendon tissue during degradation/regeneration

- **Materials**

For each material, the evolution of tensile strength and Young's Modulus throughout time was modelled by calculating regression equations with time as predictor of property.

An example of this procedure is shown in Figure 10. The values of Young's Modulus of PDS during degradation (shown in table 6) were retrieved from [143]. This was followed by the calculation of the regression model. The selection of the type of function was determined by comparing the percentage of variance explained or coefficient of determination (R^2) for linear vs higher order models and based on published results.

Table 6 - Values of Young's Modulus of PDS fibres during degradation gathered from [140]

Time (Hours)	Young's Modulus (MPa)
0	365
168	359
336	358
504	346
672	339
840	333
1008	323

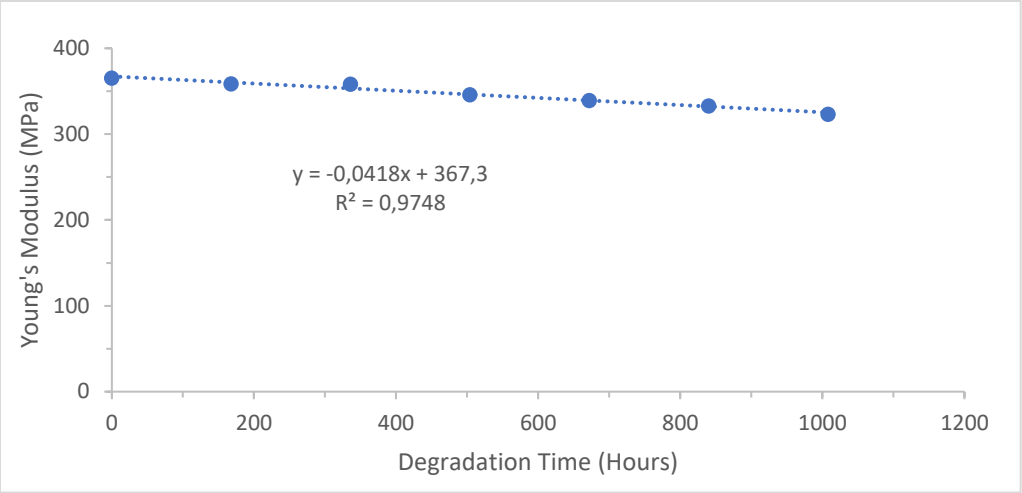

Figure 10 - Illustrative example for the modelling of Young's Modulus throughout time. In this case a linear model explains 97% of the variance of degradation.

The equations obtained thus describe the evolution of each property with time. This process was repeated to model the evolution of Young's Modulus and tensile strength of all the materials used. The evolution of the properties of the all the materials were modelled using linear or exponential functions. The regression models for the mechanical properties of the materials are shown in Annex A.

- **Regenerating tissue**

To obtain the functions regarding the regeneration of the tissue and its properties, the same method was used, with one additional feature. Limits were applied to the functions to avoid continuous growth. The limits applied are based on published results regarding the properties of the Achilles tendon after two years of healing from a total rupture [145]. In this work, these values are assumed to represent full regeneration. The evolution of Young Modulus with time, during the regeneration of tendon tissue, was modelled following the same reasoning. 369MPa was considered the upper value (withdrawn from [145]), therefore the initial Young's Modulus is of 0MPa and increases until 369MPa. The regression model used, and the evolution of the Young's Modulus can be seen in Figures 11 and 12, respectively.

For the cross-section area the same process was applied. In this case, studies indicate that the evolution throughout time is not linear, but rather best described as a quadratic function (increase followed by decrease) [148, 149]. For this reason, a polynomial trendline was used. As before, a limit was also applied (obtained from [145]) to avoid continuous evolution.

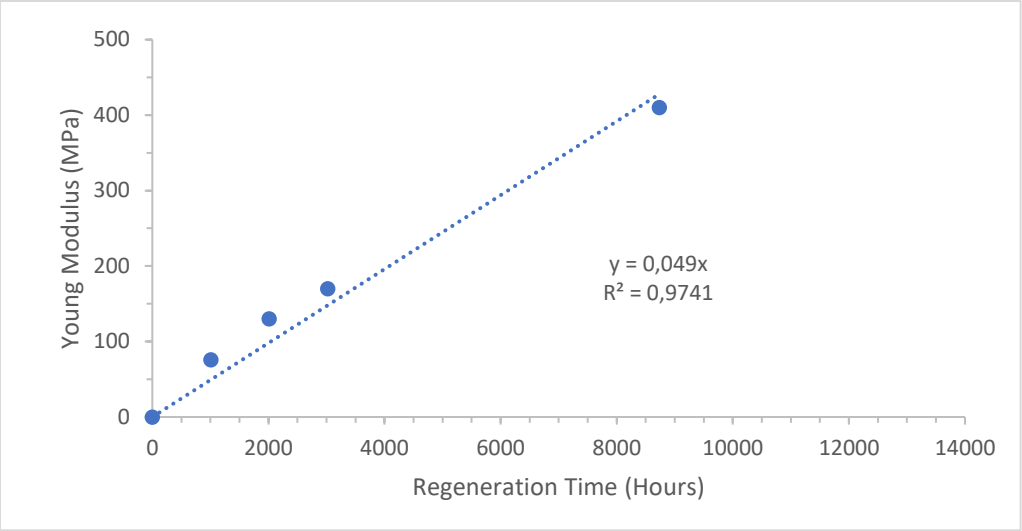

Figure 11 - Linear regression model using the data gathered of the Young's Modulus for the Achilles tendon during regeneration

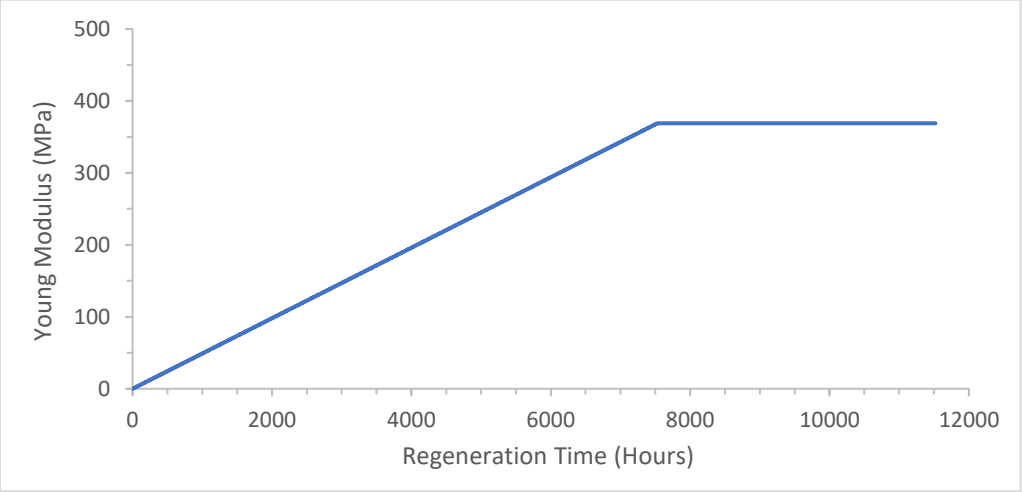

Figure 12 - Evolution of the Young's Modulus of the Achilles tendon during regeneration using the regression model and considering the assumed limit

The simulated evolution of the cross-section area is in agreement to what was found in the literature [148, 149] as it increases greatly and then, decreases after a few months until it stabilizes to a value higher than of a normal Achilles tendon. One important issue here is that the values of cross-section area gathered for this work were obtained from a study where a ruptured tendon is repaired via surgery where the two ends are sutured, and a localized callus is formed. If the measurements of the cross-section area were performed in the zone where the callus is formed, the cross-section area obtained may not represent the cross-section of the whole tendon. In our case, the equation that was obtained from the regression model, generated unrealistic results. Due to this, the mathematical expression was multiplied by a factor of 0.5, which resulted in an evolution of the parameters closer to what was

found in the literature [145]. The regression model used, and the evolution of the cross-section area is shown are shown in Figures 13 and 14 respectively.

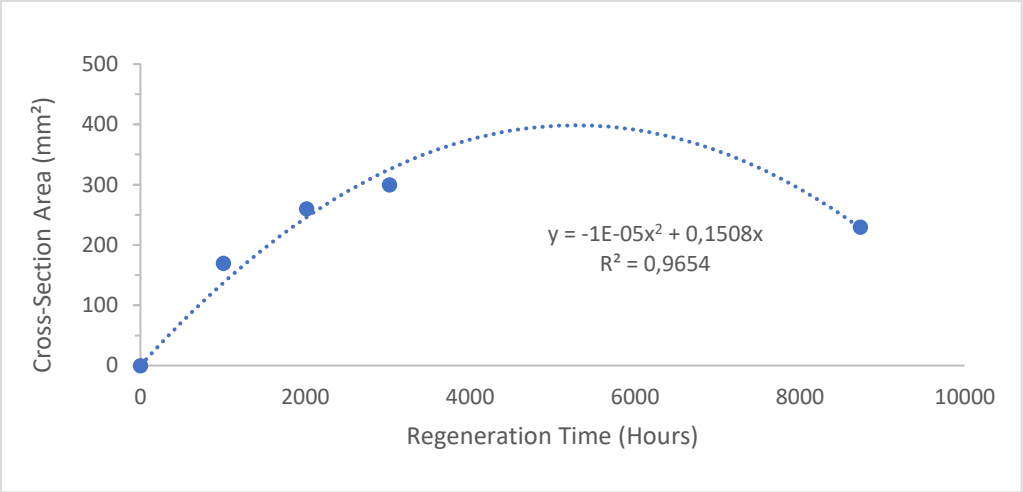

Figure 13 - Regression model obtained using the data gathered of the cross-section area for the Achilles tendon during healing from a rupture

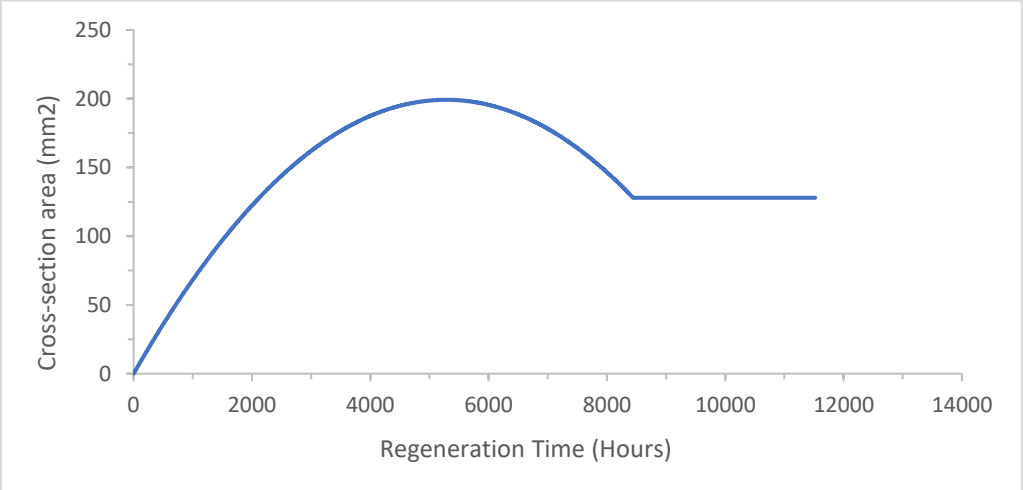

Figure 14 - Evolution of the cross-section area during regeneration using the regression model and considering the assumed limit

As for the evolution of the breaking tensile strength during regeneration of the Achilles tendon after rupture and the value of breaking tensile strength of a fully healed Achilles tendon after rupture, no data was found. Due to this, making assumptions regarding the evolution of the tensile strength and the value of breaking tensile strength of the fully healed Achilles tendon tissue was necessary. It was assumed that the tensile strength of the tissue had the same behaviour as the Young's Modulus, being directly proportional. Therefore, as the Young's Modulus of the Achilles tendon after two years of regeneration is close to half of the value for the

uninjured Achilles tendon, the same situation was assumed to happen for the tensile strength.

Therefore, if the tensile strength of a healthy Achilles tendon is 86MPa, as shown in table 5, it was assumed that for the regenerating tendon, the tensile strength increases up to 43MPa (which is half of the tensile strength of a healthy Achilles tendon found in [146]) and then ceases to evolve. Since the time needed for the Young's Modulus to reach its maximum value was close to one year, the same interval of time was set for the tensile strength of the regenerating tissue to reach its peak. The model for the evolution of the breaking tensile strength of the regenerating tendon was calculated using two points only, the initial value (σ_r=0MPa) and the tensile strength after one year of regeneration (σ_r=43MPa), which is maximum value. The model obtained using this process is shown in Figure 15.

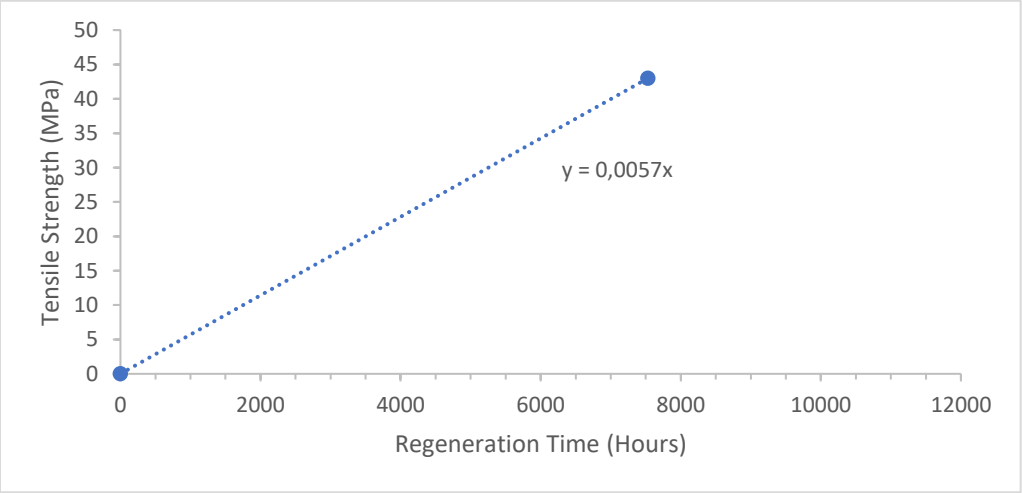

Figure 15 - Method used to obtain the model for the tensile strength of the Achilles tendon during regeneration

This equation was used to simulate the evolution of the tensile strength of the regenerating tissue. After reaching 43MPa, it does not develop further. Equations 7, 8 and 9 were obtained and translate the evolution of the tensile strength, Young's Modulus and cross-section area of the tissue, respectively.

$$\sigma_{r\text{-}tissue} = 0.0057t \quad (7)$$

$$E_{tissue} = 0.049t \quad (8)$$

$$A_{tissue} = (-1.4E\text{-}05t^2 + 0{,}1508t) \times 0.5 \quad (9)$$

The evolution of the tensile strength of the regenerating tissue is shown in Figure 14.

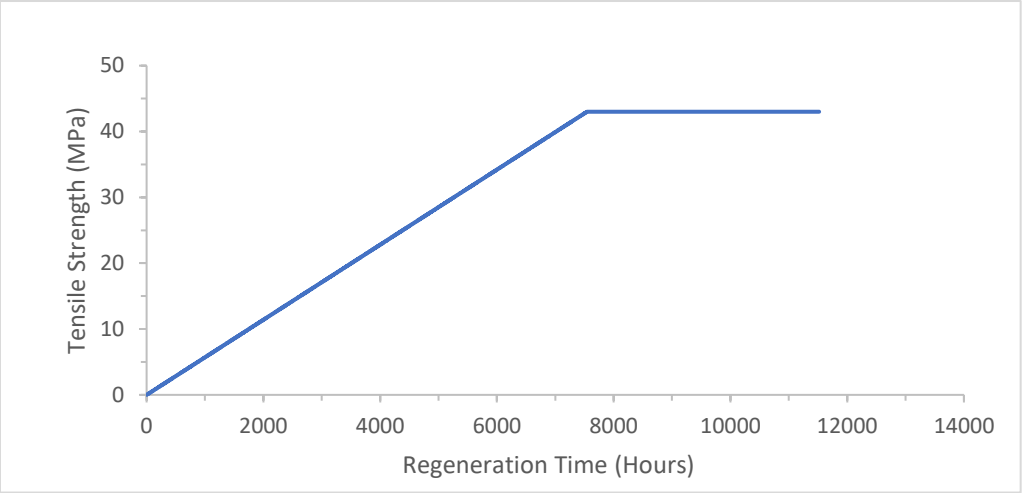

Figure 16 – Evolution of the tensile strength obtained using the regression model and the assumed limit

Due to the model used to define the evolution of the tensile strength being calculated based on assumptions only, it was necessary to investigate if there is some information that could corroborate the assumption made.

A study concerning the regeneration of the Achilles tendon in rabbits was found [46]. To validate the model used for the evolution of the tensile strength in this work, another model was built, for comparison purposes, using the information obtained from the study regarding the evolution of the tensile strength of the Achilles tendon during healing. This model exhibited a high coefficient of determination (R^2=0.91), thus corroborating, to a certain level, the type of function (linear) used to model the evolution of tensile strength in this work. The model is shown in Figure 17.

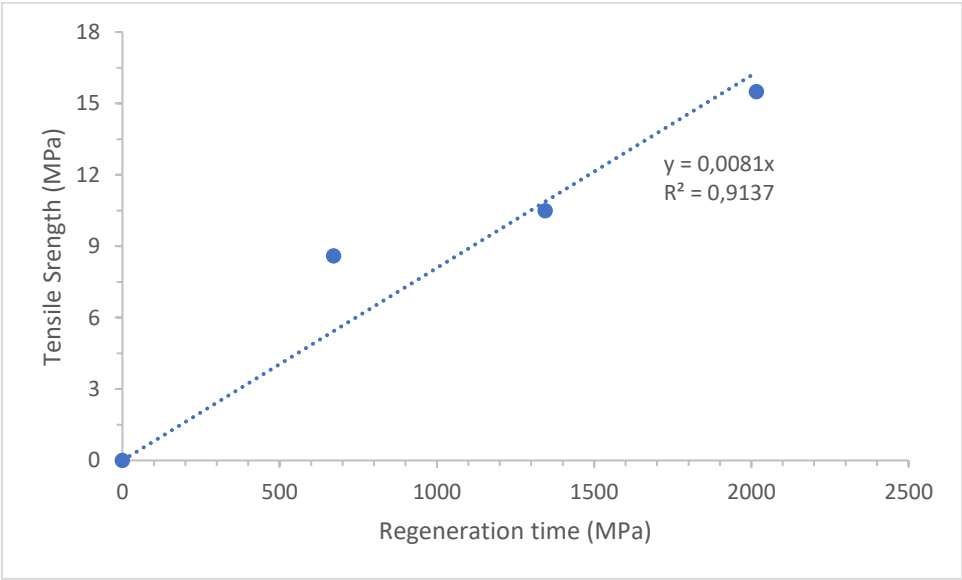

Figure 17 - Model obtained for comparison regarding the evolution of tensile strength from [43]

In another attempt to validate the assumptions made, this time to verify the value which was assumed to be the limit of the evolution of the tensile strength of tendon after healing (43MPa), a study in a sheep model, also regarding the regeneration of the Achilles tendon was considered [148]. It was observed that after one year of healing of a total rupture, the Achilles tendon exhibited a tensile strength of 56.7% of the value for the healthy tendon. This legitimizes, to some extent, the assumption made, since our hypothesis suggests that the tensile strength of the Achilles tendon regenerates until 50% of the healthy tendon value. Due to lack of information, the assumptions referred previously were necessary to enable the development of a model regarding the evolution of the tensile strength to allow the construction of the simulation. A large difference is not detected when comparing the results.

While these comparisons cannot ensure that the model used for the evolution of the tensile strength is close to the real evolution, they suggest that the probability of the model being completely unrealistic is quite low.

5.5. Scaffold Design

The design of the scaffolds consisted in determining its composition and its structure. The structure of this simplified model is formed by parallel fibres aligned in the direction of loading, as shown in Figure 20. This simple architecture is stripped from structural complexity, which simplifies the equations equilibrium deduced to correlate forces and displacements.

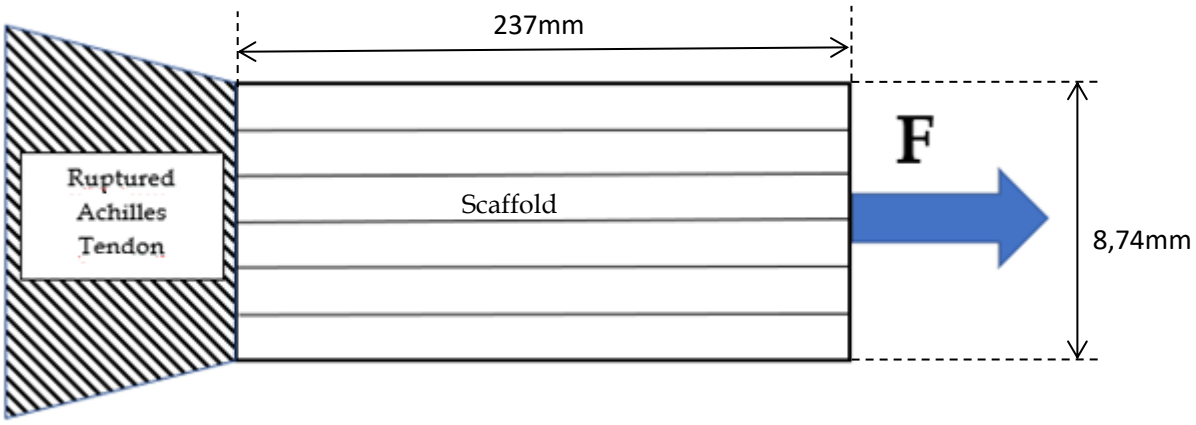

Figure 18 - Illustration of the scaffold's architecture

The composition of the scaffold is achieved through calculations to obtain the desired mechanical behaviour. The procedures were based on the Young's Modulus of the fibres and the initial stiffness which was defined for the scaffold. Some

characteristics of the scaffold were defined in advance i.e. the scaffold's Young's Modulus, length, cross-section area and the diameter of the fibres. These values were stipulated to be close to the characteristics of a healthy Achilles tendon represented in table 7. The diameter of the fibres was chosen to be similar to the collagen fibres diameter found in [150]. It was assumed that all the fibres had the same diameter with purpose of simplification. The initial Young's Modulus of the scaffold was defined to be 1000MPa, which is roughly 18% higher than a healthy Achilles tendon (according to [145]), in order to provide support to the regenerating tissue in the earlier stages.

Table 7 - Characteristics of the scaffolds

Scaffold Characteristics	**Value**
Length (mm)	237
Cross-section area (mm^2)	60
Young's Modulus (MPa)	≈1000
Fibre Diameter (mm)	0.03

As stated in [5], the stiffness of the scaffold should be designed according to the natural tissue in its linear region. In such approach, the scaffold had the form of a braided cord that, depending on the twist, could replicate the stiffness in the toe region. In this work, the toe region will not be considered, as it will be assumed that the natural tissue has a linear elastic behaviour. Despite the difference of the architectures, the same process can be applied to calculate the modulus of the structure. The modulus of the scaffold can be calculated through the law of mixtures.

The stresses in the fibrous structure can be calculated if some assumptions are made:

- All fibres extend the for same amount i.e. the length of the scaffold;
- All fibres are aligned in the direction of loading;
- The materials have a linearly elastic behaviour;
- There are no void spaces between fibres;
- The load is equally shared by the fibres i.e. proportional to stiffness;

The load sustained by the fibrous structure is given by:

$$P_{scaffold} = \sum_{i=1}^{n} P_i \tag{10}$$

with $P_{scaffold}$ representing the load supported by the scaffold and P_i representing the load supported by the fibres of the materials.

Since in tensile load $P_{scaffold} = \sigma_{scaffold} \times A_{scaffold}$, and medium stress $\sigma_{scaffold} \times A_{scaffold} = \sum_{i=1}^{n} \sigma_i \times A_i$ where σ_i is the stress supported and A_i the cross-section area of the fibres of a material.

Assuming the isostrain condition, it is obtained that:

$$\varepsilon_{scaffold} = \varepsilon_1 = \varepsilon_2 = \cdots = \varepsilon_i \tag{11}$$

With $\varepsilon_{scaffold}$ representing the strain of the scaffold and $\varepsilon_1, \varepsilon_2, \varepsilon_i$ representing the strain of the fibres of the materials.

Through the division of eq. 2 and 3, and since Young's Modulus $E = \frac{\sigma}{\varepsilon}$:

$$E_{scaffold} A_{scaffold} = \sum_{i=1}^{n} E_i A_i \tag{12}$$

With $E_{scaffold}$ representing the Young's Modulus and $A_{scaffold}$ representing the cross-section area of the scaffold and E_i representing the Young's Modulus and A_i representing the cross-section area occupied by the fibres of the materials.

As the fibres have the same length and cross-section area, then the cross-section area of each fiber will equal its respective volume fraction (V_i):

$$E_{scaffold} = \sum_{i=1}^{n} E_i V_i \tag{13}$$

Knowing the initial Young's Modulus of each material that composes the scaffold, this method allowed the calculation of the appropriate volume fraction of each material so that the scaffold could possess the desired Young's Modulus.

Since the voids between fibres are not being accounted for, therefore the number of fibres that form the scaffold ($Nf_{scaffold}$) may be given by the division between the cross-section area of the fibre (A_{fibre}) and the initial cross-section area of the scaffold ($A_{scaffold}$).

$$Nf_{scaffold} = A_{fibre} / A_{scaffold} \tag{14}$$

The number of fibres of each material (Nf_i) can be obtained by multiplying the volume fraction of the material in the scaffold for the total number of fibres in the scaffold.

$$Nf_i = V_i \times Nf_{scaffold} \quad (15)$$

Whenever the number of fibres is not an integer, the value was rounded up to the next integer.

Through these calculations the volume fractions of each material were achieved. The characteristics of the scaffolds are shown in tables 8 and 9.

- Degradable scaffold properties

Table 8 - Characteristics of the degradable scaffold

Properties	**Value**
Initial Young's Modulus (MPa)	1077
Total number of fibres	84883
Number of fibres - PLGA	21221 (Vol. fraction PLGA=0.25)
Number of fibres - PDS	35650 (Vol. fraction PDS=0.42)
Number of fibres - PLA-PCL	28012 (Vol. fraction PLA-PCL=0.33)

- Semi-Degradable scaffold Properties

Table 9 - Characteristics of the semi-degradable scaffold

Properties	**Value**
Initial Young's Modulus (MPa)	1000
Total number of fibres	84883
Number of fibres - PLGA	11884 (Vol. fraction PLGA=0.14)
Number of fibres - PDS	38197 (Vol. fraction PDS=0.45)
Number of fibres - PTFE	34802 (Vol. fraction PLA-PCL=0.41)

The polymers selected to compose the scaffolds were chosen based on their mechanical properties and their degradation rates. The scaffolds are constituted by fibres of three different materials, with different Young's Modulus and degradation rates. Each scaffold is composed by fibres with relatively low stiffness (PDS), medium (PLGA) and high stiffness (PLA-PCL for the degradable and PTFE for the semi-degradable scaffold). This provides a versatile mechanical behaviour to the scaffold, as it is composed by materials with different mechanical properties. The different degradation rates presented by the polymers indicate that they will rupture in different stages. This is a crucial aspect in the design of the scaffold, in order for

the load transference from the scaffold to the tissue to be gradual. The volume fractions of the polymers were calculated as a function of the Young's Modulus of the fibres in order for the load to be distributed throughout the fibres. If the stiffest material of the scaffold presents a very high volume fraction, this means that, at the time when the fibres of that material rupture, the high amount of load supported by these fibres would instantly be transferred to the tissue (and other fibres if they did not rupture at that time), thus leading to an abrupt load transference. The volume fraction of the non-degradable portion of the semi-degradable scaffold (PTFE) was calculated to fix the Young's Modulus of the set at values closer to a healthy Achilles tendon (≈600MPa) after the degradation of the degradable polymers.

5.6 Simulation

In the simulation, the expressions which deliver the evolution of the mechanical properties of the regenerating tissue and the materials as a function of time were applied. Through the evolution of the properties of the materials, the behaviour of the scaffold could be modelled and plotted with the growth of the regenerating tissue. More specifically, by the relationship between these properties and other parameters, such as load supported and strain, these quantities could be calculated for the elements in the simulation. These quantities will be referred further with their respective calculation method. This allowed the observation of how the scaffold would perform and if it is fulfilling its goal of supporting the tissue mechanically or if the regenerating tissue is being excessively loaded due to poor reinforcement and fails.

The degradable and semi-degradable scaffolds were simulated in the isostrain and the isostress condition. This results in different methods of calculation of the parameters and different parameters to be calculated. For example, in the isostrain condition, the load generated by strain of the elements is calculated. While in the isostress condition, the strain provoked by the load in the elements is calculated. Therefore, in the calculation methods, there are parameters which are only calculated to one of the conditions. The values of constant force and strain are shown in table 10.

Table 10 - Conditions applied to the scaffolds in the simulation

Condition	Value
Isostrain – Constant strain	0.03
Isostress – Constant force (N)	2200

These values were based on the force and elongation experienced by the Achilles tendon during walking at a speed of 0.75m/s. The method used to obtain these values was Direct Tendon estimation [21].

After setting the initial conditions, the calculations proceed to determine the forces acting on the fibres, on the tissue and on the scaffold during the regeneration of the tendon, for each time step. For calculation purposes, in the simulation, four elements were distinguished: the materials, the regenerating tissue, the scaffold and the whole set. The materials represent the polymer fibres used to build the scaffold. In this instance, the calculations were grouped individually for each polymer type. The regenerating tissue is the regenerating Achilles tendon tissue whose mechanical properties are expected to increase. The scaffold consists on the whole structure which is formed the materials, thus the calculations are made by grouping the fibres by material type. Afterwards, the set is the union between the scaffold and the regenerating tissue, which supports all the external load.

It is important to differentiate inputs and outputs. Inputs include information that is inserted such as the cross-section area occupied by the fibres of each material, the mechanical properties evolution functions, volume fraction of each material, constant strain and constant stress. Outputs are information that is obtained from the simulation, such as load and strain supported by the elements. The outputs obtained through the simulation are presented below along with their respective calculation method. These parameters were calculated for each time step.

- **Materials**

For the materials (PLA-PCL, PLGA, PDS, and PTFE), the **Maximum load**, **Total load**, **effective load**, **cross-section area** and **Young's Modulus** × **Cross-section area** were calculated.

- Failure load - $Pmax_i$

Failure load of the material i ($Pmax_i$) at a given time step was obtained by multiplying the tensile strength at the same time step by the initial cross-section area of the material i ($A0_i$). The initial cross-section area occupied by the fibres of the material i is given by the multiplication of the initial cross-section of the scaffold ($A0_{scaffold}$) by the volume fraction of the material (V_i).

$$A0_i = V_i \times A0_{scaffold} \quad (16)$$

$$Pmax_i = \sigma_i\,(t) \times A0_i \quad (17)$$

- Total load – P_i

The total load of the supported by the fibres of a material was calculated by multiplying the initial cross-section area of the material i, imposed strain and the Young's modulus of the material at that time step:

$$P_i = E(t) \times A0_i \times \varepsilon \quad (18)$$

- Effective load – Pef_i

The effective load is a condition used to define if the fibres were intact or if they ruptured due to excessive loading. If the load supported by the fibres of a material is lower than their failure load ($P_i < Pmax_i$), then $Pef_i = P_i$. On the other hand, if the load supported by the fibres is greater than their failure load ($P_i > Pmax_i$), then $Pef_i = 0$ which means the fibres of the material i ruptured.

- Cross-section area – A_j

This condition was used to define the cross-section area as function of time, because when the fibres of a material break, the cross-section area occupied by the fibres cannot be accounted for. Therefore, if the fibres of the material i have failed ($Pef_i=0$), this condition takes the value of zero. If ($Pef_i > 0$), it takes the value of the initial cross-section area occupied by the fibres of the material i.

- Young's Modulus × Cross-section area – EA_j

This parameter was used to further determine the load supported by the scaffold. It was calculated by the multiplication of two functions of time, the Young's Modulus and the cross-section area.

$$EA_i = E_i(t) \times A_i(t) \tag{19}$$

- **Regenerating tissue**

For the **regenerating tissue**, parameters such as **Maximum load**, **Total load**, **Effective load** and **Young's Modulus x Cross-section area** were determined for each time step. The Young's Modulus, Tensile strength and cross-section area of the regenerating tissue were obtained previously in section 5.4.

- Failure load - $Pmax_{tissue}$

Failure load of the regenerating tissue was calculated by the division of the tensile strength of the tissue and its cross-section area as shown in eq. 13:

$$Pmax_{tissue} = \sigma_{r-tissue}(t) \times A_{tissue}(t) \tag{20}$$

- Total load - P_{tissue}

Total load supported by the regenerating tissue was obtained by multiplying the Young's Modulus and cross-section area of the tissue and the imposed strain as in eq. 14:

$$P_{tissue} = E_{tissue}(t) \times A_{tissue}(t) \times \varepsilon \tag{21}$$

- Effective load - Pef_{tissue}

The effective load of the tissue is a condition identical as the one used for the materials. If $Pmax_{tissue} > P_{tissue}$, then $Pef_{tissue} = P_{tissue}$. If $Pmax_{tissue} < P_{tissue}$, then $Pef_{tissue}=0$

- Young's Modulus x Cross-section area - EA_{tissue}

Young's Modulus x Cross-section area of the regenerating tissue by multiplying the Young's Modulus of the tissue by its cross-section area.

$$EA_{tissue} = E_{tissue}(t) \times A_{tissue}(t) \tag{22}$$

- **Scaffold**

For the scaffold, the evolution of **total load**, **Young's modulus**, **total stress** and **cross-section area** were calculated. As said previously, the total load supported by

the scaffold equals the sum of the load supported by each fiber. The properties of the scaffold are calculated combining the parameters of the fibres. The strain (in the isostress condition) is not calculated for the scaffold, as it is not the scaffold that regulates the strain, it is the sum of the scaffold and the regenerating tissue (set).

- Total load - $P_{scaffold}$

The total load of the scaffold was calculated by sum of the loads supported by the fibres.

$$P_{scaffold} = \sum_{i=1}^{n} Pef_i \tag{23}$$

- Cross-section area - $A_{scaffold}$

The cross-section area of the scaffold was calculated by the sum of the cross-section areas of the materials, as shown in Eq. 16.

$$A_{scaffold} = \sum_{i=1}^{n} A_i \tag{24}$$

- Young's Modulus - $E_{scaffold}$

The Young's Modulus of a scaffold was calculated by the sum of the Young's Modulus of each material multiplied by the fraction between the cross-section area of the material and the cross-section area of the scaffold at that time step:

$$E_{scaffold} = \sum_{i=1}^{n} E_i \times \frac{A_i}{A_{scaffold}} \tag{25}$$

- **Set (Scaffold plus regenerating tissue)**

The parameters of the whole set (scaffold plus regenerating tissue) were calculated. Parameters such as total load, Young modulus, cross-section area, strain were calculated.

- Cross-section area - A_{set}

The cross-section area of the set is equal to the sum of the cross-section area of the scaffold and the cross-section area of the regenerating tissue.

$$A_{set} = A_{scaffold} + A_{tissue}(t) \quad (26)$$

- Young's Modulus - E_{set}

The Young's Modulus is obtained by multiplying the sum of the multiplication between the Young's Modulus of the scaffold and the fraction between the cross-section area of the scaffold and the cross-section area of the set and the multiplication between the Young's Modulus of the fraction between the cross-section area of the regenerating tissue and the cross-section area of the set.

$$E_{set} = E_{scaffold} \times \frac{A_{scaffold}}{A_{set}} + E_{reg.tissue} \times \frac{A_{tissue}(t)}{A_{set}} \quad (27)$$

- Total load - P_{set} (Isostrain condition)

The total load of the set was obtained by multiplying the strain and the sum of the Young's Modulus × Cross-section area of each material and the regenerating tissue.

$$P_{set} = \varepsilon_0 \times \left(EA_{tissue} + \sum_{i=1}^{n} EA_i \right) \quad (28)$$

- Strain - ε (Isostress condition)

The strain of the set is calculated by the division of the load supported by the scaffold and the tissue and sum of Young's Modulus × Cross-section area of the materials and the regenerating tissue:

$$\varepsilon = \frac{P_0}{EA_{tissue} + \sum EA_i} \quad (29)$$

- Stiffness - S_{set}

The stiffness of the set is calculated by the load supported by the set and the displacement produced, as shown in Eq. 30

$$S_{set} = \frac{P_{set}}{L \times \varepsilon} \quad (30)$$

The calculation scheme was different for both conditions. For the isostrain condition, the procedure was simple. First, every parameter regarding the materials was calculated as well as the parameters for the regenerating tissue. The calculations of the materials led to the calculations of the scaffold which, then led to the calculations of the set.

For the isostress condition, the same did not happen. In the isostrain condition, the strain is given as a constant condition, which makes it possible to calculate the total load and consequently the "Effective load" (parameter which indicates the breakage of the materials) of the materials before calculating the parameters for the other elements.

In the isostress condition, the force is given as a constant, thus the calculation of the strain of the set is necessary to then determine the total load and effective load supported by the fibres. Therefore, the evolution of the Young's Modulus x Cross-section area of the fibres of each material and the regenerating tissue were calculated to determine the evolution of the Young's Modulus of the set and its strain. Only then, the total load and effective load of each fibre were calculated. The fact that the strain of the set is calculated through the Young's Modulus and cross-section area of the materials to, then, calculate the load supported by each fibre indicates that the loads supported by the fibres are interdependent. This relationship between the fibres allows the study of the transference of load between fibres and tissue.

This brings one problem to the simulation. The value of effective load supported by each material is calculated using the strain of the set. However, the value of the strain also should depend on the effective load of the materials i.e., the effective load determines when fibres of a material rupture, and when this happens, it has an impact on the strain due to lesser material supporting the load. Obviously, when these interdependences are introduced in the spreadsheet, it generates an error due to circular referencing (cell trying to calculate itself). So, if the effective load is simply the condition that returns zero when the load supported by the fibres is greater than its failure load, for the simulation to work with without errors, it was necessary to determine the point when the load supported by the fibres of a material exceeds its failure and change the Young's modulus of the material in question to zero, manually. This was done for all materials. As for the regenerating tissue, it followed the same procedure to inspect if it had ruptured. Diagrams illustrating the steps followed to perform the simulation in the Isostress and in the Isostrain condition are presented in Annex B.

6. Results and discussion

6.1 Degradable Scaffold

- **Isostress**

In the isostress condition simulation, the scaffolds are subjected to a constant load of 2200N. This condition allows the study of a fundamental aspect: the load transference from the degrading scaffold to the regenerating tissue. The load should be gradually transferred to the tissue, as it regenerates, and at the point that the scaffold loses its properties and all the load is transferred to the tissue, the properties of the tissue should have already developed enough for the tissue to withstand the load fully. Because the amount of load supported each fibre is dependant of its stiffness, the Young's Modulus of the scaffold must be well adjusted.

As can be seen is figure 19, the Young's Modulus of the scaffold is initially close to 1000MPa, as established in Section 5.5, and shows an increase with time. This is due to the rupture of the fibres, first of PLGA and then of PDS. As these polymers have a lower Young's Modulus than the PLA-PCL fibres, when they rupture, the Young's Modulus of the structure increases as the scaffold is composed by stiffer fibres only. In figure 20, the Young's Modulus of the set is shown, it exhibits a major decrease in the first 1400 hours (58 days) due to the degradation of the mechanical properties of the polymers. It then stabilizes due to the balance between the degradation of the polymers and the increase of the tissue's mechanical properties.

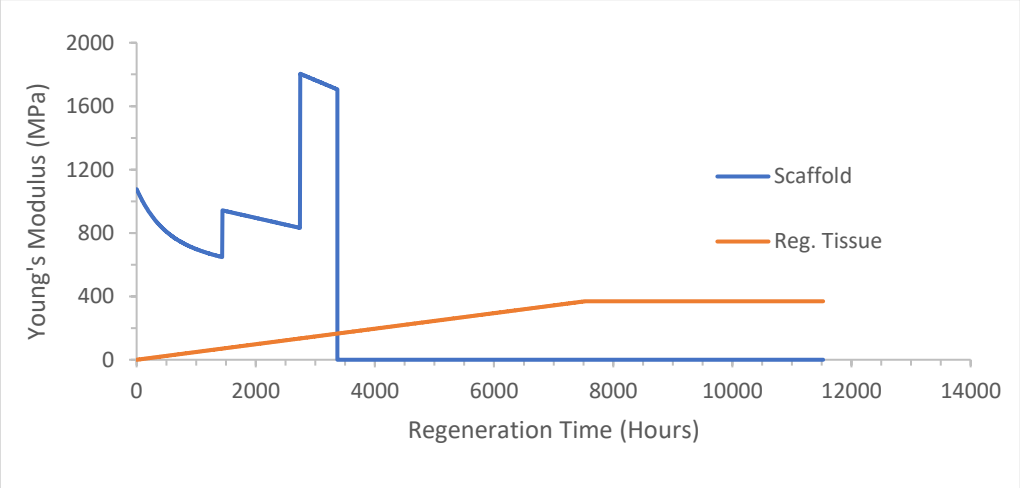

Figure 19 - Evolution of the Young's Modulus of the degradable scaffold and the regenerating tissue

Figure 20- Evolution of Young's Modulus of the set using the degradable scaffold during regeneration

The parameter exhibited in Figure 21 is the "Effective load" of the tissue. This parameter, as explained in Section 5.6, controls the breakage of elements by reducing the load to zero if, at some point, the load supported by the element surpasses the maximum load that the element can undergo. Therefore, by analysing the evolution of the load on the tissue, it can be concluded that the scaffold adequately provided mechanical support to the tissue, as it prevented the tissue from rupturing at any point, especially in the early stages of regeneration.

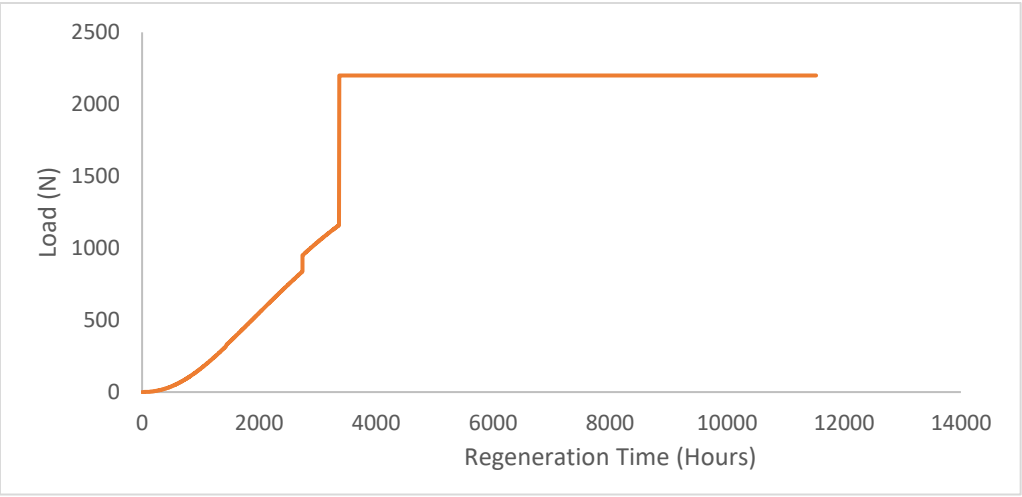

Figure 21- Evolution of the load supported by the regenerating tissue during the degradation of the degradable scaffold

In Figure 22, the transference of load from the scaffold to the tissue is shown. It is possible to observe that the load is gradually transferred to the tissue until the rupture of the scaffold. At that point, the tissue is already able to withstand the load fully.

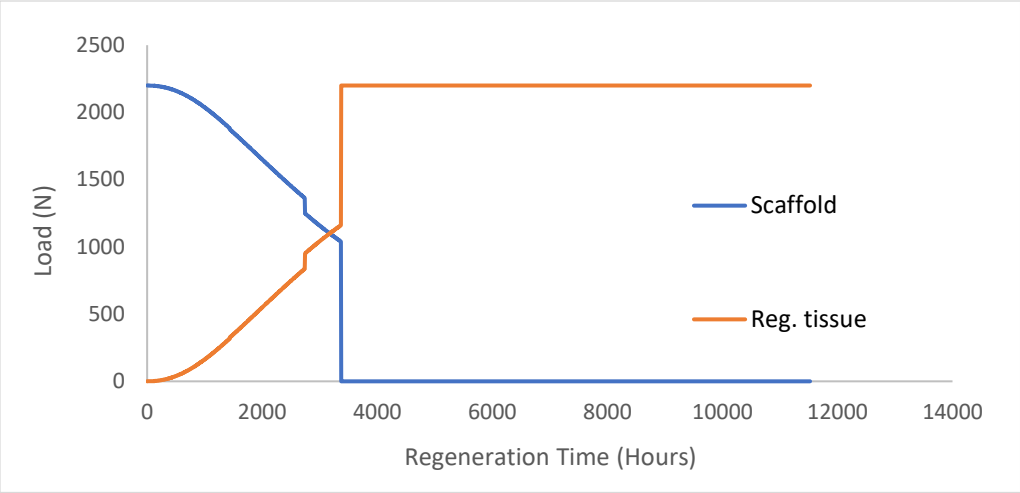

Figure 22 - Evolution of the load supported by the degradable scaffold and the regenerating tissue

As expected, a symmetry is obtained because, obviously, when the load decreases on one element, it increases the same amount on the other.

In Figure 23, the evolution of the strain of the set is represented. The strain is a function of the Young's Modulus and the cross-section area and its evolution can be explained by the evolution of these parameters.

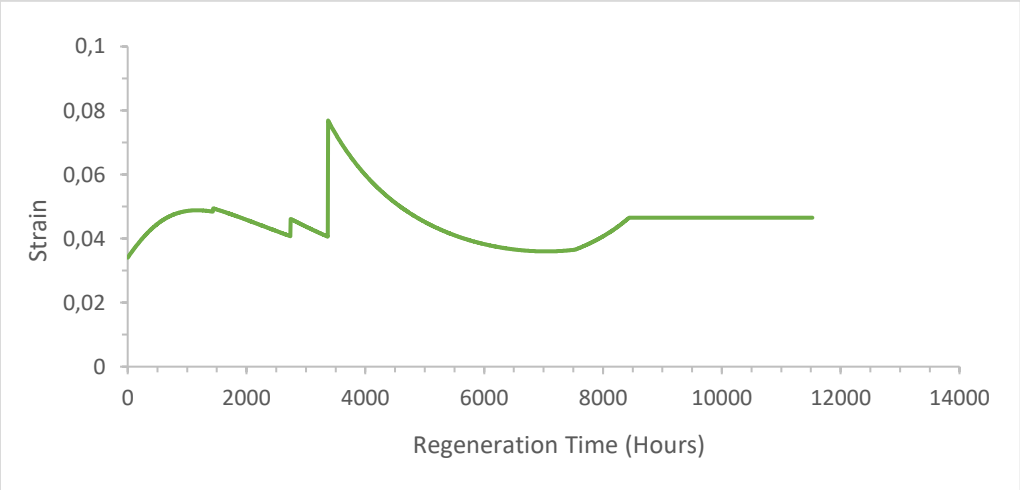

Figure 23 - Evolution of the strain of the set using the degradable scaffold

Until approximately 750 hours, an increase in strain can be seen, which is caused by the decrease of the Young's Modulus of the polymers due to degradation. This results in the decrease of the Young's Modulus of the set. The following decrease in strain, from 1500 to 3300h (except for a minor raise at 2900h due to the rupture of PDS fibres), is explained by the increase of the Young's Modulus and cross-section area of the regenerating tissue. At this point, the scaffold is losing its properties and the tissue is increasing its properties. Therefore, the evolution of the strain of the set is

regulated by the balance between the loss of properties of the scaffold and the increase of properties of the tissue. Not only the Young's Modulus of the tissue is increasing, the cross-section area is also increasing, which affects the strain of the set directly.

The rupture of the fibres at 3372h results in the peak strain of 8%. Afterwards, the strain still exhibits some variation which is connected to the fact that the Young's Modulus of the tissue is still increasing, and the cross-section area is decreasing. After 7500h, the Young's Modulus of the tissue already stabilized thus the evolution of the strain is controlled entirely by the decrease of the cross-section area of the tissue.

In Figure 24, the stiffness of the set is shown. The rupture of the fibres of each material are easily identifiable. The values of stiffness do not vary greatly except for the rupture of PLA-PCL, when a significant drop in occurs, at 3372 hours. These substantial variations are not desired and should be avoided if possible. The tissue recovers afterwards and stabilizes at values close of a healthy tendon (see table 5). Analysing the stiffness and the Young's Modulus of the fully regenerated tissue, it can be observed that the Young's Modulus decreases to less than half of a healthy tendon, but its stiffness does not experience the same variation. This suggests that the decrease in the modulus of the tissue is balanced by the increase in cross-section area of the regenerating tendon.

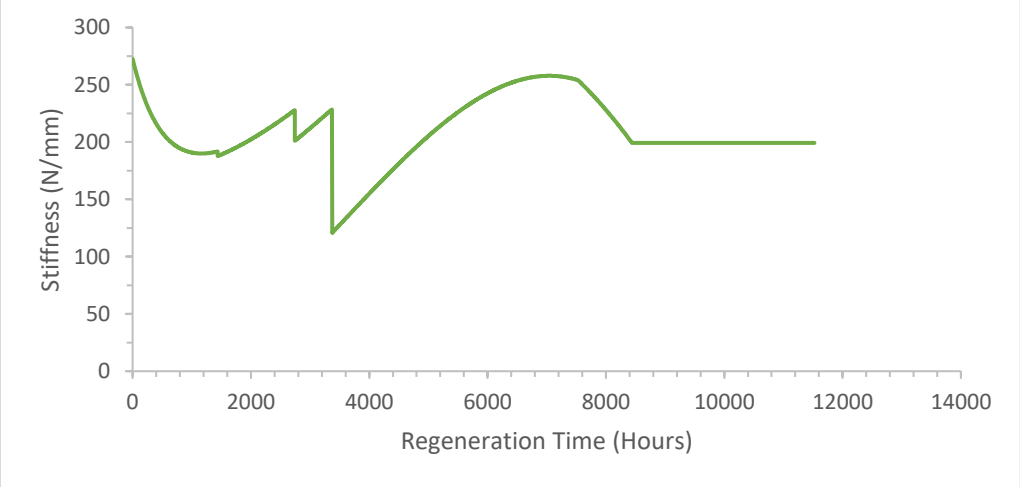

Figure 24 - Evolution of the stiffness of the set using the degradable scaffold

- **Isostrain**

In the isostrain condition all elements are strained equally, which means that the load supported by each fibre is independent of the load supported by the other fibres or tissue. The load supported by the fibres and tissue depends solely on their Young's Modulus, cross-section area and their evolution with degradation time. This is clear through analysis of the equation used to calculate loads in the isostrain condition, since the load is given by the multiplication of the strain (constant) and the Young's Modulus and the cross-section area. The simulation in isostrain condition allows the study of the loads generated by the scaffold and the tendon under a strain level associated with normal locomotion in the Achilles tendon.

For the isostrain condition, the results for the evolution of the Young's Modulus and stiffness of the scaffold and the set were almost identical with only difference being that the scaffold ruptured 10 days earlier. Since the load experienced by the fibres is independent of the load sustained by the other fibres, the presence of the scaffold does not affect the load supported by the regenerating tissue. However, studying the force generated in the scaffold and in the regenerating tissue as a function of their Young's Modulus is of interest, as well as if they fail under this level of strain.

In Figure 25, the force generated in the regenerating tissue and the scaffold is shown.

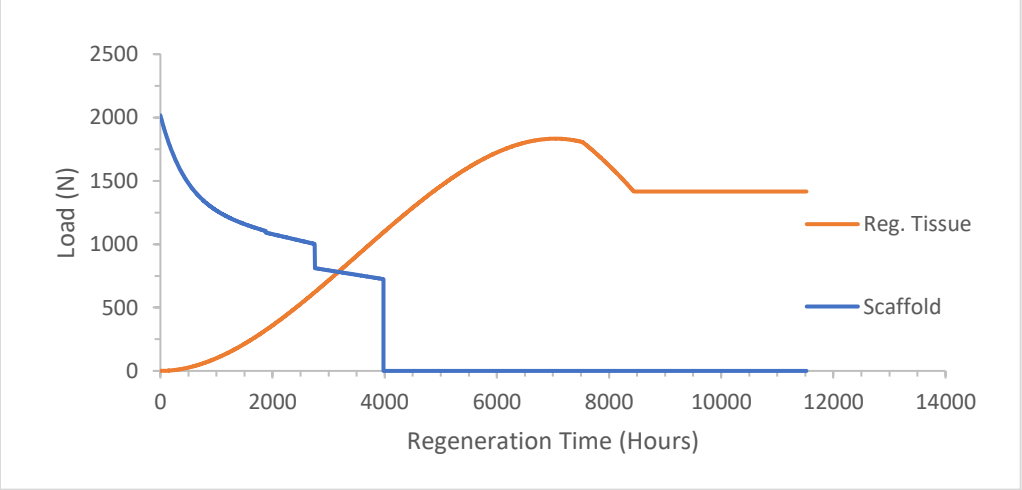

Figure 25 – Evolution of the load supported by the regenerating tissue and the degradable scaffold in the isostrain condition

The load on the tissue increases with time, as a function of its modulus, reaching 1850N and then decreases again due to the decrease in cross-section area. The tissue endured the strain without breaking, which means that it can be exposed to strains associated with walking without rupturing.

In Figure 26, the load supported by the set can be seen. The rupture of the PDS and PLA-PCL fibres are clear, as well as the effect of the evolution of the Young's Modulus and the cross-section area of the regenerating tissue. The Young's Modulus increases until approximately 7000h. This leads to an increase in the load generated in the tissue in that period of time followed by a decrease which is the result of the reduction of the cross-section area of the tissue, since it is the only parameter which, at that time point, is still evolving.

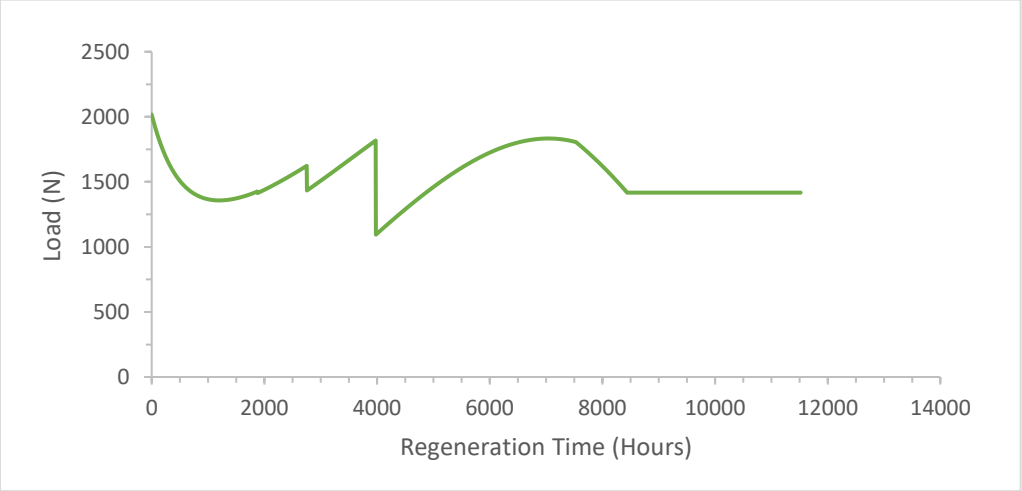

Figure 26 - Evolution of the load supported by the set using the degradable scaffold in the isostrain condition

6.2 Semi-Degradable scaffold

- **Isostress**

As can be seen in Figure 27, the semi-degradable scaffold, exhibits two sudden increases, in its Young's Modulus, at 1600h and 2700h, due to the rupture of PLGA and PDS fibres respectively. The Young's Modulus of the scaffold stabilizes at 1656MPa, where the scaffold is composed only by the non-degradable portion, PTFE. In this case, as the scaffold is not completely degradable, the regenerating tissue never supports the load fully, as the PTFE does not degrade and keep its mechanical properties constant.

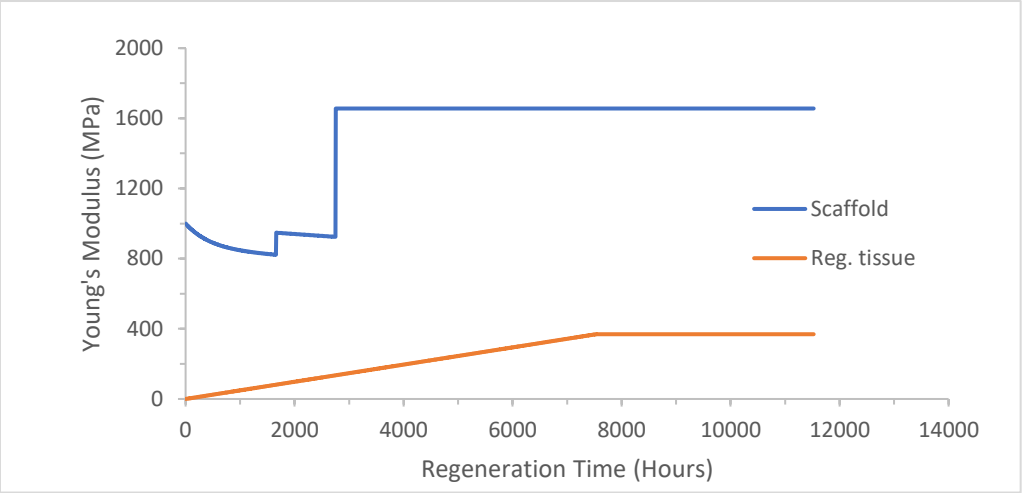

Figure 27 - Evolution of the Young's Modulus of the semi-degradable scaffold and the regenerating tissue in the isostress condition

In Figure 28, the Young's Modulus of the set is shown.

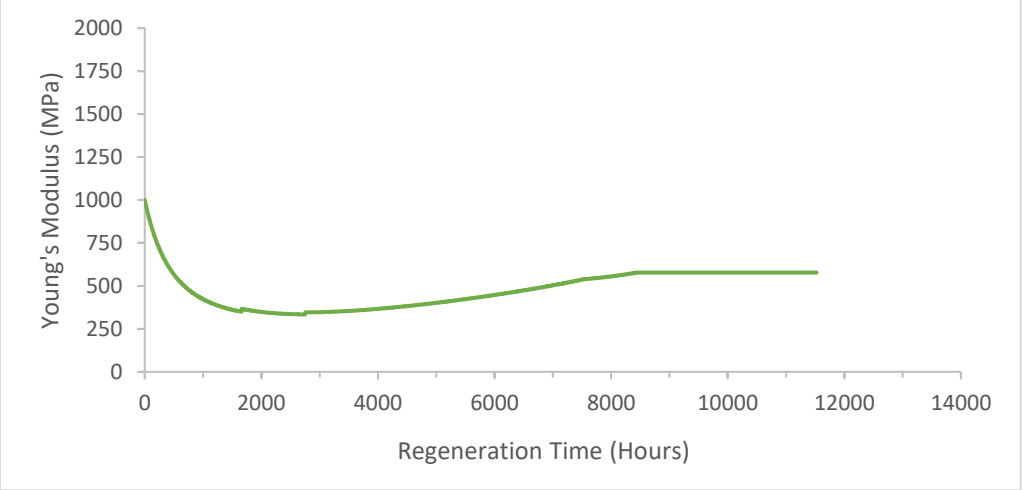

Figure 28 - Evolution of Young's Modulus of the set using the semi-degradable scaffold in the isostress condition

Even though that the scaffold has an increase in its modulus, the set decreases its modulus due to the low modulus of the regenerating tissue at that point. Later, the modulus begins to increase with the increase in the tissue and stabilizes after, at 577MPa. When compared to the modulus of the tissue after total regeneration, it is approximately 1.5 times higher.

The stiffness of the set is shown in Figure 29. Employing the semi-degradable scaffold, the set does not exhibit significant drops in its stiffness. This behaviour is preferred over the slightly more irregular evolution shown with the degradable scaffold. However, the values of stiffness using the semi-degradable scaffold are considerably higher than of a healthy Achilles tendon, hence becoming susceptible to stress-shielding.

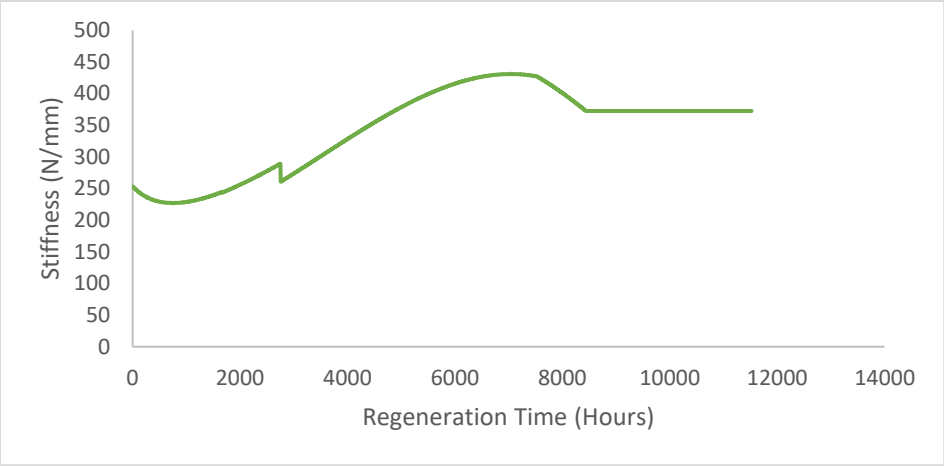

Figure 29 - Evolution of the stiffness of the set using the semi-degradable scaffold in the isostress condition

In Figure 30, the load supported by the regenerating tissue is shown.

Figure 30 - Evolution of the load supported by the regenerating tissue in the isostress condition using the semi-degradable scaffold

The load supported by the tissue has a gradual increase and stabilizes afterwards. In this case, after the degradation of PDS and PLGA the amount of load that the tissue must bear is much lower than in the scenario using the degradable scaffold. By having PTFE as a permanent reinforcement, the load is divided between PTFE and the tissue, leaving the tissue to withstand only 55% of the total load. The load supported by the scaffold and the tissue is shown in Figure 31.

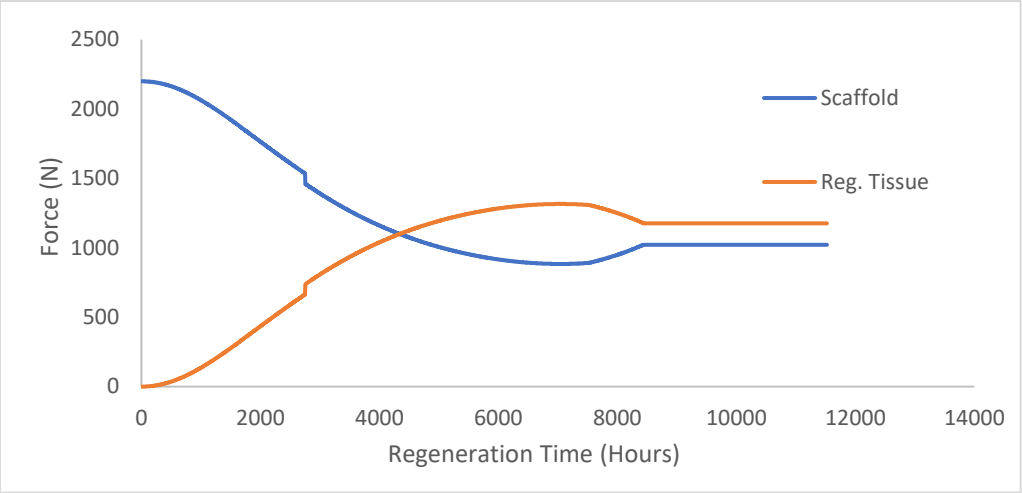

Figure 31 - Evolution of the load supported by the regenerating tissue and the semi-degradable scaffold in the isostress condition

In Figure 32, the strain of the set is shown.

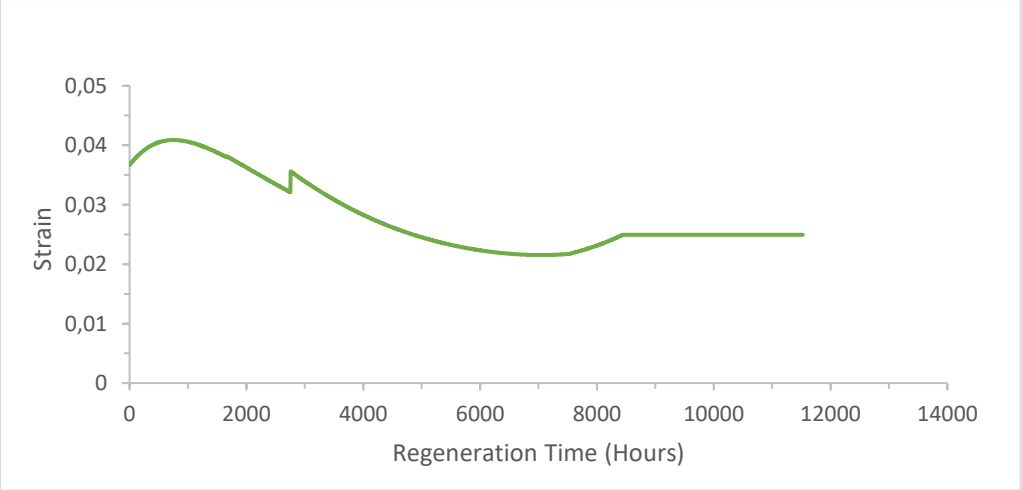

Figure 32 - Evolution of the strain of the set using the semi-degradable scaffold in the isostress condition

When compared to the strain of the set using the degradable scaffold, this set displays approximately half of the peak strain with 4% at approximately 750h, then stabilizing at 2.5% after the tissue regenerates completely. As expected an inverse proportionality is clear between the stiffness and strain of the set.

- **Isostrain**

As said earlier, when in the isostrain condition, the reinforcement of the scaffold has no effect on the load supported by the regenerating tissue, therefore the load supported by the regenerating tissue is equal as with the degradable scaffold, as can be seen in Figure 33.

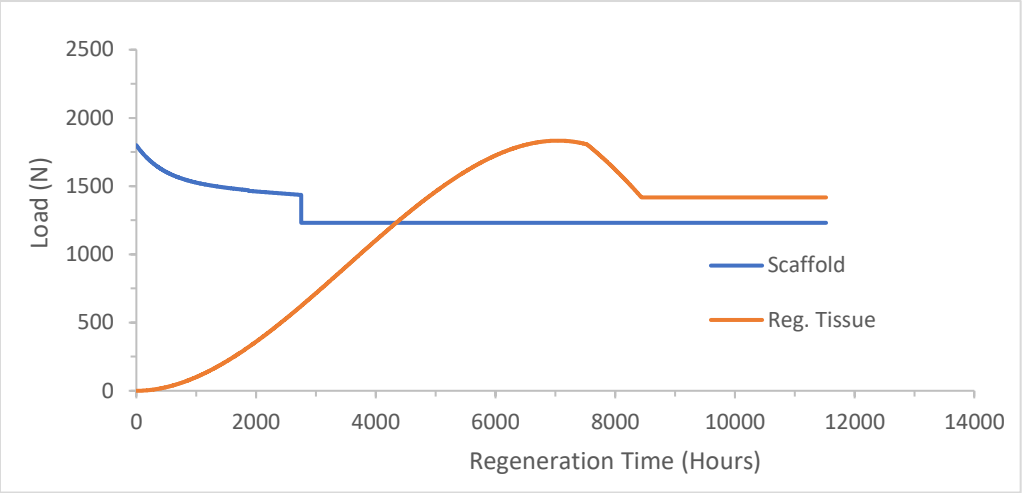

Figure 33 - Evolution of the load supported by the regenerating tissue and the semi-degradable scaffold

In Figure 34, the load supported by the set is shown. As can be seen, there is a considerable increase in the load provoked by the strain. This is a result of the increase both of cross-section area and the Young's Modulus of the regenerating tissue.

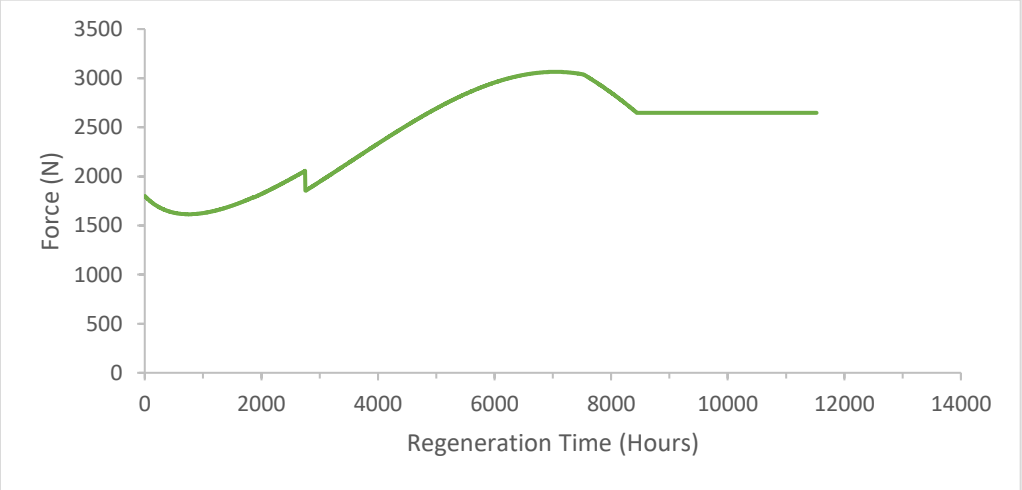

Figure 34 - Evolution of the load supported by the set using the semi-degradable scaffold in the isostrain condition

Being this a simplified model, the results obtained cannot describe real, *in vivo* conditions. However, it is possible to state that the scaffolds presented adequate mechanical behaviour during degradation under the simulation conditions. The devices provided support to the regenerating tissue in the earlier stages, preventing early rupture, then degrading gradually and transferring the load to the tissue. In the case of the degradable scaffold, the rupture of the device occurred properly i.e. it lost its properties when the mechanical properties of the regenerating tissue already permitted full load withstanding, without rupturing.

This suitable behaviour is a result of the polymers used to compose the scaffold and the respective volume fractions. Therefore, the compositions of the degradable and semi-degradable scaffold seemed promising for future investigation. It is important to mention that the values of the mechanical properties of the polymers were withdrawn from the literature and are concerning different fibre diameters. It was assumed that changing the fibre diameter to the diameter used in the scaffolds (30μm) would not affect the mechanical properties. Presumably, this will not happen. In addition to this, the degradation rates of the fibres will also vary when using different diameters due to surface area/volume ratio alterations.

This investigation was also an attempt to better understand the behaviour of the tissue and the scaffold while degrading and how transference of load would happen. Avoiding the phenom of stress shielding was attempted designing a scaffold with a Young's Modulus proximate to the healthy Achilles tendon tissue, but it was not possible to find if stress-shielding would occur or not. Information which could aid in predicting if stress-shielding would occur in this case was not found in the literature. Much work is yet to be done in this field such as defining and quantifying the growth rate of tissues in the presence of a scaffold, the evolution of the properties of the scaffold while performing, the properties of the tissue after total regeneration using a scaffold and defining the ideal properties of the scaffold each application such as cross-section area, tensile strength and Young's Modulus.

Both scaffolds, degradable and semi-degradable, performed well. The indicator for the performance of the scaffold is the load supported by the regenerating tissue, which shows if it ruptured due to overload or not. Another aspect that is important to mention is that it was assumed that the properties of the tendon after regeneration through scaffolding were the same as after regeneration through a suturing surgery. Even though some studies about the mechanical properties of the regenerating Achilles tendon *in vitro* and in animal models were found and an approximation could be made to the human Achilles tendon, it was chosen to utilize data regarding the regenerating human Achilles tendon through suturing surgery.

Differences between the isostrain and isostress condition were noticeable on obtained results. The independence of the loads supported between fibres in the isostrain condition was evident by comparing the loads supported by the tissue when

using the degradable and the semi-degradable scaffold. The scaffolds had different evolutions in their modulus, but the evolution of the load supported by the tissue was identical.

In theory, the semi-degradable scaffold would be more advantageous due to its continued support to the weaker tissue. However, the use of non-degradable polymers in ligament and tendon grafts has shown many disadvantages including the presence of wear debris, loss of mechanical properties, stress-shielding and more. Therefore, the application of semi-degradable scaffolds, could be a promising solution but only if the limitations of the employment of non-degradable polymers in artificial ligaments and tendons were solved.

7. Model limitations

The limitations of this model reside on the simplifications which were employed to perform the simulation and the design. Mimicking the behaviour of materials *in vivo* and the growth and healing of a ligament or tendon is always very complex, due to the number of variables on which the healing process depends and to the *in vivo* environment. These simplifications include assumptions which had to be made to perform the simulation and approximations due to lack of information and data.

Regarding the design of the scaffold, these include, the structure of the scaffold, the material properties and their degradation in materials and the mechanical behaviour of the materials. The structure of the scaffold utilized in this work consisted on parallel fibres with no voids between fibres. This architecture was chosen to simplify the algorithmic procedure used in the simulation. The scaffolds have many requirements about their structure such as high porosity and high surface to volume ratio which were not considered in model. Another characteristic that was assumed to simplify calculations is that the elements exhibit a linear elastic behaviour. This is a simplification, as polymers and the tendinous tissue display viscoelastic behaviour. Another limitation is the suitability of the data chosen to represent the properties of the elements. The mechanical properties were gathered from literature, in different degradation media and their evolution was obtained by extrapolation and interpolation. The degradation studies of all the materials used were performed *in vitro* and not *in vivo* which also affects the accuracy of the data used for this application. Also, regarding the degradation of the fibres, it was

assumed that all the fibres experience degradation equally. *In vivo* this is not likely to occur as polymeric fibres exhibit variations in their properties from fibre to fibre and not all the fibres in the scaffold have equal exposure to the degradation medium.

In the simulation there are some limitations as well. Firstly, in the obtention of the data. Like in the materials, the growth of the tendon and its mechanical properties are an approximation to reality. The functions which represent the evolution of the mechanical properties of the regenerating tissue were obtained also by an extrapolation of data from another study, with low data volume. This limits the ability of the function to approximate itself from the reality. This lack or low volume of data to extrapolate from is especially critical in the case of the tensile strength of the regenerating tissue where assumptions had to be made in order to model its evolution based on two points. Furthermore, the study used to represent the mechanical evolution of the regenerating tissue regards Achilles tendon ruptures which were repaired by suturing the ends of the tendon. The healing process in this case is surely different than using a scaffold for tendon repair. While the suturing of the tendon leads to scarring of the tissue, the use of a scaffold induces a process which relies more on tissue growth rather than scarring. This impacts the characteristics of the tendon such as its morphology and mechanical properties. Another limitation in this simulation are the efforts endured by the tendon and the materials. In the simulation performed in this investigation, materials and tendon undergo constant stress and strain to study its behaviour during the degradation of the polymers and the growth of the tendon. This does not correspond to reality where the tendons are subjected to cyclic efforts. All these simplifications and assumptions affected the results obtained. By simplifying the design of the scaffold to parallel fibres only with no voids or porosity, a difference in the mechanical properties is obtained. In the simulation, it is assumed that the cross-section area of the scaffold is entirely composed by material, which is not what happens when using fibrous scaffolds. Fibrous scaffolds generally exhibit high porosity, which results in lower mechanical properties when compared to low or zero porosity structures. In addition to this, functional Achilles tendon scaffolds for application *in vivo* are generally utilized in the form of knitted or braided structures, rather than parallel fibres. This also affects the mechanical properties of the scaffold, because changing the

structure results in a variation of the stiffness, tensile strength and maximum elongation of the scaffold, due to each structure having its characteristics.

Regarding the simplification that both, the polymers and the regenerating tissue, exhibit a linear elastic behaviour rather than a viscoelastic behaviour, impact the results since in the simulation isostrain and isostress conditions were applied. If the viscoelastic properties of the elements would have been considered, the constant stress applied to the elements would not result in a constant strain of the elements but in a strain, which would vary with time. The same case applies to the isostrain condition, where the constant strain applied would result in a varying stress depending on time in the elements.

Concerning the use of material degradation studies in *in vitro* conditions, this affects results by obtaining lower material degradation rates than in *in vivo* conditions. *In vivo* conditions involve the presence of enzymes, which increase polymer degradation. This increase depends on the degree to which polymers suffer enzymatic degradation. As PLGA and PDS are not affected greatly by enzymatic activity, a large increase would not be expected. As for PLA-PCL, both polymers show higher degradation rates in the presence of certain enzymes, therefore a faster degradation could occur.

In relation to the data regarding the regeneration of the Achilles tendon being from studies where the tendon was repaired by suturing the tendon rather than being treated with the use of a scaffold, the healing process differ as said previously, and based on the study in a rabbit model from Moshiri et al. [151], the mechanical properties of the tendon should recover at a higher rate and reach higher values when treated with scaffolds than when treated with a simple suture of both ends of the tendon.

Lastly, the evolution of the mechanical properties of the materials and regenerating tissue were obtained through extrapolation and interpolation using a low amount of data, which may impact the accuracy of the functions obtained.

8. Conclusions

Despite being a simplified model, this work allowed the attainment of some insight regarding the mechanical behaviour of a scaffold and the regenerating tissue during healing of an Achilles tendon rupture. More specifically, it permitted the study of the degradation of a scaffold at the same time as the regeneration of the Achilles tendon tissue and in what manner the transference of the load could occur. In this simulation, the designed scaffolds proved to be suitable, in the mechanical aspect, for use in an Achilles tendon rupture site. However, much research needs to be done to confirm if these scaffold compositions are appropriate for scaffolding in real, *in vivo* conditions.

The hypothesis of the employment of a semi-degradable scaffold was proposed, due to the low mechanical properties exhibited by the tendon after full regeneration. However, the increase in cross-section area observed in the fully regenerated tendon appears to balance the low mechanical properties of the tissue by maintaining the stiffness and maximum load at values not too far from a healthy tendon. This suggests that using a non-degradable portion to reinforce the tendon permanently may not be necessary. Further research must be done to confirm the validity of this assertion.

Much work is yet to be done in the field of tissue engineering, particularly on the mechanical aspects, such as defining the mechanical properties of the Achilles tendon after full healing of a total rupture and studying the evolution of those mechanical properties during regeneration. For instance, data regarding the breaking tensile strength of tendons after rupture was not found in the literature. Another important aspect to be studied is the treatment of this injury using tissue engineering scaffolds and the effect of these devices on the mechanical properties of the regenerating tendon.

Following this work, more accurate simulations can be performed. This can be accomplished by using a fibrous structure suitable for scaffolding combined with Finite Element Method in the simulation. This would also be achieved if the degradation tests are performed at similar conditions to the *in vivo* environment. Filling the gaps of information detected during this investigation, would also avoid some *a priori* simplifications and assumptions.

9. References

1. Robi, K., et al., *The physiology of sports injuries and repair processes*, in *Current issues in sports and exercise medicine*. 2013, InTech.
2. Thayer, P. and A. Goldstein, *Bio-Instructive Scaffolds for Tendon/Ligament Regeneration*, in *Bio-Instructive Scaffolds for Musculoskeletal Tissue Engineering and Regenerative Medicine*. 2017, Elsevier. p. 87-112.
3. Yang, G., B.B. Rothrauff, and R.S. Tuan, *Tendon and ligament regeneration and repair: clinical relevance and developmental paradigm.* Birth Defects Research Part C: Embryo Today: Reviews, 2013. **99**(3): p. 203-222.
4. Hauser, R.A. and E.E. Dolan, *Ligament injury and healing: an overview of current clinical concepts.* Journal of Prolotherapy, 2011. **3**(4): p. 836-846.
5. Vieira, A., R. Guedes, and A. Marques, *Development of ligament tissue biodegradable devices: a review.* Journal of biomechanics, 2009. **42**(15): p. 2421-2430.
6. Morais, D., et al., *Current approaches and future trends to promote tendon repair.* Annals of biomedical engineering, 2015. **43**(9): p. 2025-2035.
7. James, R., et al., *Tendon: biology, biomechanics, repair, growth factors, and evolving treatment options.* The Journal of hand surgery, 2008. **33**(1): p. 102-112.
8. Legnani, C., et al., *Anterior cruciate ligament reconstruction with synthetic grafts. A review of literature.* International orthopaedics, 2010. **34**(4): p. 465-471.
9. Liu, Y., H. Ramanath, and D.-A. Wang, *Tendon tissue engineering using scaffold enhancing strategies.* Trends in biotechnology, 2008. **26**(4): p. 201-209.
10. Chan, B. and K. Leong, *Scaffolding in tissue engineering: general approaches and tissue-specific considerations.* European spine journal, 2008. **17**(4): p. 467-479.
11. Rathbone, S. and S. Cartmell, *Tissue Engineering of Ligaments*, in *Tissue Engineering for Tissue and Organ Regeneration*. 2011, InTech.
12. Sharma, P. and N. Maffulli, *Biology of tendon injury: healing, modeling and remodeling.* Journal of Musculoskeletal and Neuronal Interactions, 2006. **6**(2): p. 181.
13. Frank, C., *Ligament structure, physiology and function.* Journal of Musculoskeletal and Neuronal Interactions, 2004. **4**(2): p. 199.
14. Hampson, K., et al., *Tendon tissue engineering.* Topics in tissue engineering, 2008. **4**.
15. Harvey, A., et al., *Functional imaging of tendon.* Ann. Brit. Machine Vision Assoc, 2009. **2009**: p. 1-11.
16. Fung, Y.-c., *Biomechanics: mechanical properties of living tissues*. 2013: Springer Science & Business Media.
17. Jung, H.-J., M.B. Fisher, and S.L. Woo, *Role of biomechanics in the understanding of normal, injured, and healing ligaments and tendons.* BMC Sports Science, Medicine and Rehabilitation, 2009. **1**(1): p. 9.
18. Sopakayang, R., *Viscoelastic Models for Ligaments and Tendons*. 2010, Virginia Tech.
19. Funk, J., et al., *Linear and quasi-linear viscoelastic characterization of ankle ligaments.* Journal of biomechanical engineering, 2000. **122**(1): p. 15-22.
20. Nunley, J.A., *The Achilles tendon: treatment and rehabilitation*. 2008: Springer.
21. Zelik, K.E. and J.R. Franz, *It's positive to be negative: Achilles tendon work loops during human locomotion.* PLoS One, 2017. **12**(7): p. e0179976.
22. Doral, M.N., et al., *Functional anatomy of the Achilles tendon.* Knee Surgery, Sports Traumatology, Arthroscopy, 2010. **18**(5): p. 638-643.
23. Kraushaar, B.S. and R.P. Nirschl, *Current concepts review-tendinosis of the elbow (Tennis Elbow). Clinical features and findings of histological, immunohistochemical, and electron microscopy studies.* JBJS, 1999. **81**(2): p. 259-278.
24. Eriksen, H.A., et al., *Increased content of type III collagen at the rupture site of human Achilles tendon.* Journal of Orthopaedic Research, 2002. **20**(6): p. 1352-1357.

25. Sharma, P. and N. Maffulli, *Tendon injury and tendinopathy: healing and repair.* JBJS, 2005. **87**(1): p. 187-202.
26. Maffulli, N., et al., *Early weightbearing and ankle mobilization after open repair of acute midsubstance tears of the Achilles tendon.* The American journal of sports medicine, 2003. **31**(5): p. 692-700.
27. Chutkan, N.B., *Surgical versus nonsurgical treatment of acute Achilles tendon rupture: a meta-analysis of randomized trials.* Orthopedics, 2013. **36**(2): p. 136-137.
28. Sorrenti, S.J., *Achilles tendon rupture: effect of early mobilization in rehabilitation after surgical repair.* Foot & ankle international, 2006. **27**(6): p. 407-410.
29. Ellenbecker, T.S., M. De Carlo, and C. DeRosa, *Effective functional progressions in sport rehabilitation*. 2009: Human Kinetics.
30. Frost, H., *Does the anterior cruciate have a modeling threshold? A case for the affirmative.* JOURNAL OF MUSCULOSKELETAL AND NEURONAL INTERACTIONS, 2001. **2**(2): p. 131-136.
31. Malaviya, P., et al., *An in vivo model for load-modulated remodeling in the rabbit flexor tendon.* Journal of Orthopaedic Research, 2000. **18**(1): p. 116-125.
32. Wang, J.H., Q. Guo, and B. Li, *Tendon biomechanics and mechanobiology—a minireview of basic concepts and recent advancements.* Journal of hand therapy, 2012. **25**(2): p. 133-141.
33. Nöth, U., et al., *Anterior cruciate ligament constructs fabricated from human mesenchymal stem cells in a collagen type I hydrogel.* Cytotherapy, 2005. **7**(5): p. 447-455.
34. Loh, Q.L. and C. Choong, *Three-dimensional scaffolds for tissue engineering applications: role of porosity and pore size.* Tissue Engineering Part B: Reviews, 2013. **19**(6): p. 485-502.
35. Yang, S., et al., *The design of scaffolds for use in tissue engineering. Part I. Traditional factors.* Tissue engineering, 2001. **7**(6): p. 679-689.
36. Cheung, H.-Y., et al., *A critical review on polymer-based bio-engineered materials for scaffold development.* Composites Part B: Engineering, 2007. **38**(3): p. 291-300.
37. Stratton, S., et al., *Bioactive polymeric scaffolds for tissue engineering.* Bioactive materials, 2016. **1**(2): p. 93-108.
38. Ratcliffe, A., et al., *Scaffolds for tendon and ligament repair and regeneration.* Annals of biomedical engineering, 2015. **43**(3): p. 819-831.
39. Discher, D.E., D.J. Mooney, and P.W. Zandstra, *Growth factors, matrices, and forces combine and control stem cells.* Science, 2009. **324**(5935): p. 1673-1677.
40. Li, W.J., R.M. Shanti, and R.S. Tuan, *Electrospinning technology for nanofibrous scaffolds in tissue engineering.* Nanotechnologies for the Life Sciences: Online, 2007.
41. Lotfi, M., M. Nejib, and M. Naceur, *Cell adhesion to biomaterials: concept of biocompatibility*, in *Advances in Biomaterials Science and Biomedical Applications*. 2013, InTech.
42. Boland, E.D., et al., *Utilizing acid pretreatment and electrospinning to improve biocompatibility of poly (glycolic acid) for tissue engineering.* Journal of Biomedical Materials Research Part B: Applied Biomaterials: An Official Journal of The Society for Biomaterials, The Japanese Society for Biomaterials, and The Australian Society for Biomaterials and the Korean Society for Biomaterials, 2004. **71**(1): p. 144-152.
43. Yang, J., et al., *Fabrication and surface modification of macroporous poly (L-lactic acid) and poly (L-lactic-co-glycolic acid)(70/30) cell scaffolds for human skin fibroblast cell culture.* Journal of Biomedical Materials Research: An Official Journal of The Society for Biomaterials, The Japanese Society for Biomaterials, and The Australian Society for Biomaterials and the Korean Society for Biomaterials, 2002. **62**(3): p. 438-446.
44. Ng, R., et al., *Three-dimensional fibrous scaffolds with microstructures and nanotextures for tissue engineering.* Rsc Advances, 2012. **2**(27): p. 10110-10124.
45. Woo, K.M., V.J. Chen, and P.X. Ma, *Nano-fibrous scaffolding architecture selectively enhances protein adsorption contributing to cell attachment.* Journal of Biomedical Materials Research Part A: An Official Journal of The Society for Biomaterials, The Japanese Society for Biomaterials, and The Australian Society for Biomaterials and the Korean Society for Biomaterials, 2003. **67**(2): p. 531-537.

46. Young, R.G., et al., *Use of mesenchymal stem cells in a collagen matrix for Achilles tendon repair.* Journal of Orthopaedic Research, 1998. **16**(4): p. 406-413.
47. Kryger, G.S., et al., *A comparison of tenocytes and mesenchymal stem cells for use in flexor tendon tissue engineering.* The Journal of hand surgery, 2007. **32**(5): p. 597-605.
48. Tan, Q., et al., *Comparison of potentials of stem cells isolated from tendon and bone marrow for musculoskeletal tissue engineering.* Tissue Engineering Part A, 2011. **18**(7-8): p. 840-851.
49. Cao, Y., et al., *Bridging tendon defects using autologous tenocyte engineered tendon in a hen model.* Plastic and reconstructive surgery, 2002. **110**(5): p. 1280-1289.
50. Deng, D., et al., *Engineering human neo-tendon tissue in vitro with human dermal fibroblasts under static mechanical strain.* Biomaterials, 2009. **30**(35): p. 6724-6730.
51. James, R., et al., *Tendon tissue engineering: adipose-derived stem cell and GDF-5 mediated regeneration using electrospun matrix systems.* Biomedical materials, 2011. **6**(2): p. 025011.
52. Vaquette, C., et al., *A poly (lactic-co-glycolic acid) knitted scaffold for tendon tissue engineering: an in vitro and in vivo study.* Journal of Biomaterials Science, Polymer Edition, 2010. **21**(13): p. 1737-1760.
53. Awad, H.A., et al., *In vitro characterization of mesenchymal stem cell-seeded collagen scaffolds for tendon repair: effects of initial seeding density on contraction kinetics.* Journal of Biomedical Materials Research: An Official Journal of The Society for Biomaterials, The Japanese Society for Biomaterials, and The Australian Society for Biomaterials and the Korean Society for Biomaterials, 2000. **51**(2): p. 233-240.
54. Chen, X., et al., *Stepwise differentiation of human embryonic stem cells promotes tendon regeneration by secreting fetal tendon matrix and differentiation factors.* Stem cells, 2009. **27**(6): p. 1276-1287.
55. Sahni, V., et al., *The role of tissue engineering in achilles tendon repair: a review.* Current stem cell research & therapy, 2015. **10**(1): p. 31-36.
56. Lee, K., E.A. Silva, and D.J. Mooney, *Growth factor delivery-based tissue engineering: general approaches and a review of recent developments.* Journal of the Royal Society Interface, 2010: p. rsif20100223.
57. Screen, H.R., et al., *Cyclic tensile strain upregulates collagen synthesis in isolated tendon fascicles.* Biochemical and biophysical research communications, 2005. **336**(2): p. 424-429.
58. Yamamoto, E., et al., *Effects of the frequency and duration of cyclic stress on the mechanical properties of cultured collagen fascicles from the rabbit patellar tendon.* Journal of biomechanical engineering, 2005. **127**(7): p. 1168-1175.
59. Juncosa-Melvin, N., et al., *Effects of mechanical stimulation on the biomechanics and histology of stem cell‐collagen sponge constructs for rabbit patellar tendon repair.* Tissue engineering, 2006. **12**(8): p. 2291-2300.
60. Garvin, J., et al., *Novel system for engineering bioartificial tendons and application of mechanical load.* Tissue engineering, 2003. **9**(5): p. 967-979.
61. Lee, J., et al., *Regeneration of Achilles' tendon: the role of dynamic stimulation for enhanced cell proliferation and mechanical properties.* Journal of Biomaterials Science, Polymer Edition, 2010. **21**(8-9): p. 1173-1190.
62. Ge, Z., et al., *Characterization of knitted polymeric scaffolds for potential use in ligament tissue engineering.* Journal of Biomaterials Science, Polymer Edition, 2005. **16**(9): p. 1179-1192.
63. Blair, T., *Biomedical Textiles for Orthopaedic and Surgical Applications: Fundamentals, Applications and Tissue Engineering*. 2015: Elsevier.
64. Lee, J.-h., et al., *Guidance of in vitro migration of human mesenchymal stem cells and in vivo guided bone regeneration using aligned electrospun fibers.* Tissue Engineering Part A, 2013. **20**(15-16): p. 2031-2042.
65. Xu, C., et al., *Aligned biodegradable nanofibrous structure: a potential scaffold for blood vessel engineering.* Biomaterials, 2004. **25**(5): p. 877-886.

66. Ouyang, H.W., et al., *Knitted poly-lactide-co-glycolide scaffold loaded with bone marrow stromal cells in repair and regeneration of rabbit Achilles tendon.* Tissue engineering, 2003. **9**(3): p. 431-439.
67. Ouyang, H.W., et al., *The efficacy of bone marrow stromal cell-seeded knitted PLGA fiber scaffold for Achilles tendon repair.* Annals of the New York Academy of Sciences, 2002. **961**(1): p. 126-129.
68. Chen, J.L., et al., *Efficacy of hESC-MSCs in knitted silk-collagen scaffold for tendon tissue engineering and their roles.* Biomaterials, 2010. **31**(36): p. 9438-9451.
69. Eichhorn, S.J. and W.W. Sampson, *Statistical geometry of pores and statistics of porous nanofibrous assemblies.* Journal of the royal society Interface, 2005. **2**(4): p. 309-318.
70. Nisbet, D., et al., *A review of the cellular response on electrospun nanofibers for tissue engineering.* Journal of biomaterials applications, 2009. **24**(1): p. 7-29.
71. Botchwey, E.A., et al., *Tissue engineered bone: Measurement of nutrient transport in three-dimensional matrices.* Journal of Biomedical Materials Research Part A: An Official Journal of The Society for Biomaterials, The Japanese Society for Biomaterials, and The Australian Society for Biomaterials and the Korean Society for Biomaterials, 2003. **67**(1): p. 357-367.
72. Tuzlakoglu, K., et al., *Design of nano-and microfiber combined scaffolds by electrospinning of collagen onto starch-based fiber meshes: a man-made equivalent of natural extracellular matrix.* Tissue Engineering Part A, 2010. **17**(3-4): p. 463-473.
73. Pham, Q.P., U. Sharma, and A.G. Mikos, *Electrospun poly (ε -caprolactone) microfiber and multilayer nanofiber/microfiber scaffolds: characterization of scaffolds and measurement of cellular infiltration.* Biomacromolecules, 2006. **7**(10): p. 2796-2805.
74. Lee, Y.H., et al., *Electrospun dual-porosity structure and biodegradation morphology of Montmorillonite reinforced PLLA nanocomposite scaffolds.* Biomaterials, 2005. **26**(16): p. 3165-3172.
75. Thorvaldsson, A., et al., *Electrospinning of highly porous scaffolds for cartilage regeneration.* Biomacromolecules, 2008. **9**(3): p. 1044-1049.
76. Jia, Y.-H. and P.-F. Sun, *Comparison of clinical outcome of autograft and allograft reconstruction for anterior cruciate ligament tears.* Chinese medical journal, 2015. **128**(23): p. 3163.
77. Chen, J., et al., *Scaffolds for tendon and ligament repair: review of the efficacy of commercial products.* Expert review of medical devices, 2009. **6**(1): p. 61-73.
78. Ibrahim, S.A.R., et al., *Surgical management of traumatic knee dislocation.* Arthroscopy: The Journal of Arthroscopic & Related Surgery, 2008. **24**(2): p. 178-187.
79. Brunet, P., et al., *Reconstruction of acute posterior cruciate ligament tears using a synthetic ligament.* 2014.
80. Lavoie, P., J. Fletcher, and N. Duval, *Patient satisfaction needs as related to knee stability and objective findings after ACL reconstruction using the LARS artificial ligament.* The knee, 2000. **7**(3): p. 157-163.
81. Matsumoto, H. and K. Fujikawa, *Leeds-Keio artificial ligament: a new concept for the anterior cruciate ligament reconstruction of the knee.* The Keio journal of medicine, 2001. **50**(3): p. 161-166.
82. Ochi, M., et al., *Arthroscopic and histologic evaluation of anterior cruciate ligaments reconstructed with the Leeds-Keio ligament.* Arthroscopy: The Journal of Arthroscopic & Related Surgery, 1993. **9**(4): p. 387-393.
83. Rading, J. and L. Peterson, *Clinical experience with the Leeds-Keio artificial ligament in anterior cruciate ligament reconstruction: a prospective two-year follow-up study.* The American journal of sports medicine, 1995. **23**(3): p. 316-319.
84. Macnicol, M., I. Penny, and L. Sheppard, *Early results of the Leeds-Keio anterior cruciate ligament replacement.* The Journal of bone and joint surgery. British volume, 1991. **73**(3): p. 377-380.

85. Matsumoto, H., et al., *Anterior cruciate ligament reconstruction and physiological joint laxity: earliest changes in joint stability and stiffness after reconstruction.* Journal of orthopaedic science, 1999. **4**(3): p. 191-196.
86. McLoughlin, S. and R. Smith, *The Leeds-Keio prosthesis in chronic anterior cruciate deficiency.* Clinical orthopaedics and related research, 1992(283): p. 215-222.
87. Tanaka, N., et al., *Augmented subscapularis muscle transposition for rotator cuff repair during shoulder arthroplasty in patients with rheumatoid arthritis.* Journal of shoulder and elbow surgery, 2006. **15**(1): p. 2-6.
88. Akali, A. and N. Niranjan, *Management of bilateral Achilles tendon rupture associated with ciprofloxacin: a review and case presentation.* Journal of Plastic, Reconstructive & Aesthetic Surgery, 2008. **61**(7): p. 830-834.
89. Usami, N., et al., *Clinical application of artificial ligament for ankle instability—long-term follow-up.* Journal of long-term effects of medical implants, 2000. **10**(4).
90. Gisselfält, K., B. Edberg, and P. Flodin, *Synthesis and properties of degradable poly (urethane urea) s to be used for ligament reconstructions.* Biomacromolecules, 2002. **3**(5): p. 951-958.
91. Liljensten, E., et al., *Studies of polyurethane urea bands for ACL reconstruction.* Journal of Materials Science: Materials in Medicine, 2002. **13**(4): p. 351-359.
92. Gretzer, C., et al., *The inflammatory cell influx and cytokines changes during transition from acute inflammation to fibrous repair around implanted materials.* Journal of Biomaterials Science, Polymer Edition, 2006. **17**(6): p. 669-687.
93. Nilsson, A., et al., *Results from a degradable TMC joint Spacer (Artelon) compared with tendon arthroplasty.* The Journal of hand surgery, 2005. **30**(2): p. 380-389.
94. Nair, L.S. and C.T. Laurencin, *Biodegradable polymers as biomaterials.* Progress in polymer science, 2007. **32**(8): p. 762-798.
95. Ulery, B.D., L.S. Nair, and C.T. Laurencin, *Biomedical Applications of Biodegradable Polymers.* Journal of polymer science. Part B, Polymer physics, 2011. **49**(12): p. 832-864.
96. Middleton, J.C. and A.J. Tipton, *Synthetic biodegradable polymers as orthopedic devices.* Biomaterials, 2000. **21**(23): p. 2335-2346.
97. Ratner, B.D., et al., *Biomaterials science: an introduction to materials in medicine*. 2004: Academic press.
98. Laycock, B., et al., *Lifetime prediction of biodegradable polymers.* Progress in Polymer Science, 2017. **71**: p. 144-189.
99. Vieira, A., et al., *4D numerical analysis of scaffolds: a new approach*, in *Tissue Engineering*. 2014, Springer. p. 69-95.
100. Lee, K.H. and C. Chu, *The role of superoxide ions in the degradation of synthetic absorbable sutures.* Journal of Biomedical Materials Research: An Official Journal of The Society for Biomaterials, The Japanese Society for Biomaterials, and The Australian Society for Biomaterials and the Korean Society for Biomaterials, 2000. **49**(1): p. 25-35.
101. Uhrich, K.E., et al., *Polymeric systems for controlled drug release.* Chemical reviews, 1999. **99**(11): p. 3181-3198.
102. Azevedo, H.S. and R.L. Reis, *Understanding the enzymatic degradation of biodegradable polymers and strategies to control their degradation rate.* Biodegradable systems in tissue engineering and regenerative medicine. Boca Raton, FL: CRC Press, 2005. **177201**.
103. Banerjee, A., K. Chatterjee, and G. Madras, *Enzymatic degradation of polymers: a brief review.* Materials Science and Technology, 2014. **30**(5): p. 567-573.
104. Gan, Z., et al., *Enzymatic degradation of poly (ε -caprolactone) film in phosphate buffer solution containing lipases.* Polymer degradation and stability, 1997. **56**(2): p. 209-213.
105. Okada, M., *Chemical syntheses of biodegradable polymers.* Progress in polymer science, 2002. **27**(1): p. 87-133.
106. P Pawar, R., et al., *Biomedical applications of poly (lactic acid).* Recent Patents on Regenerative Medicine, 2014. **4**(1): p. 40-51.

107. Bergsma, J.E., et al., *Late degradation tissue response to poly (L-lactide) bone plates and screws*, in *The Biomaterials: Silver Jubilee Compendium*. 2006, Elsevier. p. 101-107.
108. Cai, H., et al., *Effects of physical aging, crystallinity, and orientation on the enzymatic degradation of poly (lactic acid).* Journal of Polymer Science Part B: Polymer Physics, 1996. **34**(16): p. 2701-2708.
109. Li, S., et al., *Enzymatic degradation of stereocopolymers derived from L-, DL-and meso-lactides.* Polymer Degradation and Stability, 2000. **67**(1): p. 85-90.
110. Ueda, H. and Y. Tabata, *Polyhydroxyalkanonate derivatives in current clinical applications and trials.* Advanced drug delivery reviews, 2003. **55**(4): p. 501-518.
111. Kanczler, J.M., et al., *The effect of mesenchymal populations and vascular endothelial growth factor delivered from biodegradable polymer scaffolds on bone formation.* Biomaterials, 2008. **29**(12): p. 1892-1900.
112. Ma, H., J. Hu, and P.X. Ma, *Polymer scaffolds for small-diameter vascular tissue engineering.* Advanced functional materials, 2010. **20**(17): p. 2833-2841.
113. Ushida, T., et al., *Three-dimensional seeding of chondrocytes encapsulated in collagen gel into PLLA scaffolds.* Cell transplantation, 2002. **11**(5): p. 489-494.
114. Yin, Z., et al., *The regulation of tendon stem cell differentiation by the alignment of nanofibers.* Biomaterials, 2010. **31**(8): p. 2163-2175.
115. Gunatillake, P.A. and R. Adhikari, *Biodegradable synthetic polymers for tissue engineering.* Eur Cell Mater, 2003. **5**(1): p. 1-16.
116. Cai, Q., et al., *Enzymatic degradation behavior and mechanism of poly (lactide-co-glycolide) foams by trypsin.* Biomaterials, 2003. **24**(4): p. 629-638.
117. Sahoo, S., et al., *Characterization of a novel polymeric scaffold for potential application in tendon/ligament tissue engineering.* Tissue engineering, 2006. **12**(1): p. 91-99.
118. Jeong, S.I., et al., *Tissue-engineered vascular grafts composed of marine collagen and PLGA fibers using pulsatile perfusion bioreactors.* Biomaterials, 2007. **28**(6): p. 1115-1122.
119. Uematsu, K., et al., *Cartilage regeneration using mesenchymal stem cells and a three-dimensional poly-lactic-glycolic acid (PLGA) scaffold.* Biomaterials, 2005. **26**(20): p. 4273-4279.
120. Wang, Y., et al., *Degradable PLGA scaffolds with basic fibroblast growth factor: experimental studies in myocardial revascularization.* Texas Heart Institute Journal, 2009. **36**(2): p. 89.
121. Woodruff, M.A. and D.W. Hutmacher, *The return of a forgotten polymer—polycaprolactone in the 21st century.* Progress in polymer science, 2010. **35**(10): p. 1217-1256.
122. Sahoo, S., J.G. Cho-Hong, and T. Siew-Lok, *Development of hybrid polymer scaffolds for potential applications in ligament and tendon tissue engineering.* Biomedical materials, 2007. **2**(3): p. 169.
123. Dhanumalayan, E. and G.M. Joshi, *Performance properties and applications of polytetrafluoroethylene (PTFE)—a review.* Advanced Composites and Hybrid Materials, 2018: p. 1-22.
124. Sze, D.Y., et al., *Recurrent TIPS failure associated with biliary fistulae: treatment with PTFE-covered stents.* Cardiovascular and interventional radiology, 1999. **22**(4): p. 298-304.
125. Bosiers, M., et al., *Heparin-bonded expanded polytetrafluoroethylene vascular graft for femoropopliteal and femorocrural bypass grafting: 1-year results.* Journal of vascular surgery, 2006. **43**(2): p. 313-318.
126. Barber, H.D., et al., *Using a dense PTFE membrane without primary closure to achieve bone and tissue regeneration.* Journal of Oral and Maxillofacial Surgery, 2007. **65**(4): p. 748-752.
127. Glousman, R., et al., *Gore-Tex prosthetic ligament in anterior cruciate deficient knees.* The American journal of sports medicine, 1988. **16**(4): p. 321-326.
128. Indelicato, P.A., M.S. Pascale, and M.O. Huegel, *Early experience with the GORE-TEX polytetrafluoroethylene anterior cruciate ligament prosthesis.* The American journal of sports medicine, 1989. **17**(1): p. 55-62.

129. Dahlstedt, L., N. Dalén, and U. Jonsson, *Goretex prosthetic ligament vs. Kennedy ligament augmentation device in anterior cruciate ligament reconstruction: a prospective randomized 3-year follow-up of 41 cases.* Acta Orthopaedica Scandinavica, 1990. **61**(3): p. 217-224.
130. Miller, M.D., C.L. Peters, and B. Allen, *Early aseptic loosening of a total knee arthroplasty due to Gore-Tex particle‐induced osteolysis.* The Journal of arthroplasty, 2006. **21**(5): p. 765-770.
131. Roolker, W., et al., *The Gore-Tex prosthetic ligament as a salvage procedure in deficient knees.* Knee Surgery, Sports Traumatology, Arthroscopy, 2000. **8**(1): p. 20-25.
132. Boland, E.D., et al., *Electrospinning polydioxanone for biomedical applications.* Acta Biomaterialia, 2005. **1**(1): p. 115-123.
133. Goonoo, N., et al., *Polydioxanone-based bio-materials for tissue engineering and drug/gene delivery applications.* European Journal of Pharmaceutics and Biopharmaceutics, 2015. **97**: p. 371-391.
134. Sabino, M.A., et al., *Study of the hydrolytic degradation of polydioxanone PPDX.* Polymer Degradation and Stability, 2000. **69**(2): p. 209-216.
135. Muftuoglu, M.T., E. Ozkan, and A. Saglam, *Effect of human pancreatic juice and bile on the tensile strength of suture materials.* The American journal of surgery, 2004. **188**(2): p. 200-203.
136. DeOrio, J.K. and A.W. Ware, *Single absorbable polydioxanone pin fixation for distal chevron bunion osteotomies.* Foot & ankle international, 2001. **22**(10): p. 832-835.
137. Sell, S., et al., *Electrospun polydioxanone‐elastin blends: potential for bioresorbable vascular grafts.* Biomedical materials, 2006. **1**(2): p. 72.
138. Smith, M.J., et al., *Suture-reinforced electrospun polydioxanone‐elastin small-diameter tubes for use in vascular tissue engineering: a feasibility study.* Acta Biomaterialia, 2008. **4**(1): p. 58-66.
139. Lee, J.-H., et al., *Tissue-engineered bone formation using periosteal-derived cells and polydioxanone/pluronic F127 scaffold with pre-seeded adipose tissue-derived CD146 positive endothelial-like cells.* Biomaterials, 2011. **32**(22): p. 5033-5045.
140. Oryan, A., A. Moshiri, and A. Meimandi-Parizi, *Implantation of a novel tissue-engineered graft in a large tendon defect initiated inflammation, accelerated fibroplasia and improved remodeling of the new Achilles tendon: a comprehensive detailed study with new insights.* Cell and tissue research, 2014. **355**(1): p. 59-80.
141. Banks, J., *Introduction to simulation*, in *Proceedings of the 31st conference on Winter simulation: Simulation---a bridge to the future - Volume 1*. 1999, ACM: Phoenix, Arizona, USA. p. 7-13.
142. Vieira, A., *Biomechanical Simulation Modelling of Biodegradable Composites in Ligament Tissue Augmentation Devices*, in *Faculty of Engineering*. 2011. p. 227.
143. Zilberman, M., K.D. Nelson, and R.C. Eberhart, *Mechanical properties and in vitro degradation of bioresorbable fibers and expandable fiber-based stents.* Journal of Biomedical Materials Research Part B: Applied Biomaterials: An Official Journal of The Society for Biomaterials, The Japanese Society for Biomaterials, and The Australian Society for Biomaterials and the Korean Society for Biomaterials, 2005. **74**(2): p. 792-799.
144. Goessi, M., T. Tervoort, and P. Smith, *Melt-spun poly (tetrafluoroethylene) fibers.* Journal of materials science, 2007. **42**(19): p. 7983-7990.
145. Geremia, J.M., et al., *The structural and mechanical properties of the Achilles tendon 2 years after surgical repair.* Clinical Biomechanics, 2015. **30**(5): p. 485-492.
146. Wren, T.A., et al., *Mechanical properties of the human achilles tendon.* Clinical Biomechanics, 2001. **16**(3): p. 245-251.
147. Schepull, T., et al., *Mechanical properties during healing of Achilles tendon ruptures to predict final outcome: a pilot Roentgen stereophotogrammetric analysis in 10 patients.* BMC musculoskeletal disorders, 2007. **8**(1): p. 116.

148. Bruns, J., et al., *Achilles tendon rupture: experimental results on spontaneous repair in a sheep-model.* Knee Surgery, Sports Traumatology, Arthroscopy, 2000. **8**(6): p. 364-369.
149. Müller, S.A., et al., *Tendon healing: an overview of physiology, biology, and pathology of tendon healing and systematic review of state of the art in tendon bioengineering.* Knee surgery, sports traumatology, arthroscopy, 2015. **23**(7): p. 2097-2105.
150. Järvinen, T.A., et al., *Collagen fibres of the spontaneously ruptured human tendons display decreased thickness and crimp angle.* Journal of Orthopaedic Research, 2004. **22**(6): p. 1303-1309.
151. Moshiri, A., A. Oryan, and A. Meimandi-Parizi, *Role of tissue-engineered artificial tendon in healing of a large Achilles tendon defect model in rabbits.* Journal of the American College of Surgeons, 2013. **217**(3): p. 421-441. e8.

Annex A - Regression models used to obtain the mechanical properties of materials

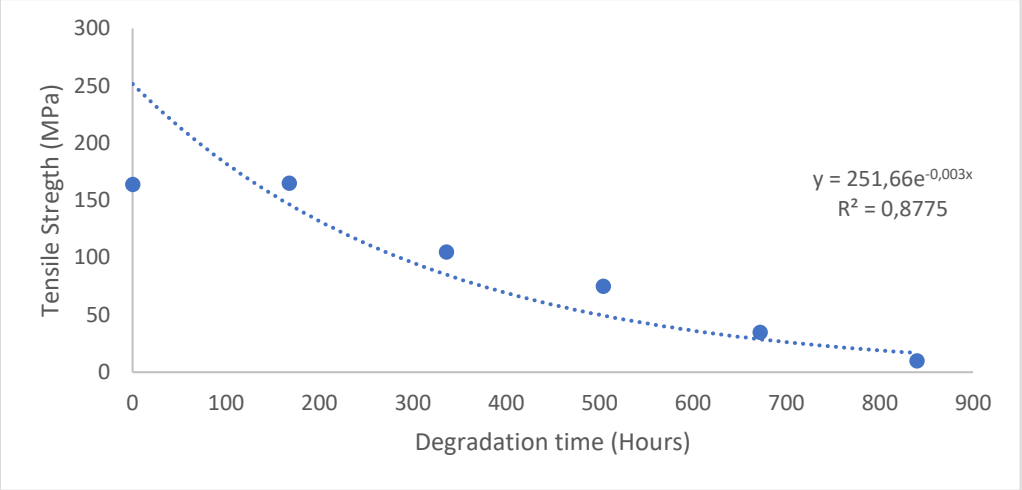

Figure 1 - Regression model used for the Tensile strength of PLGA

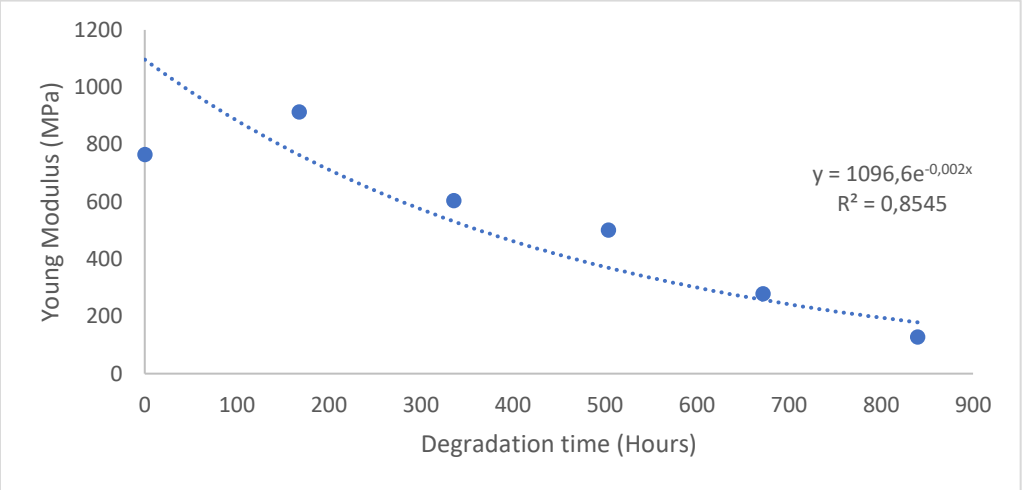

Figure 2 - Regression model used for the Young's Modulus of PLGA

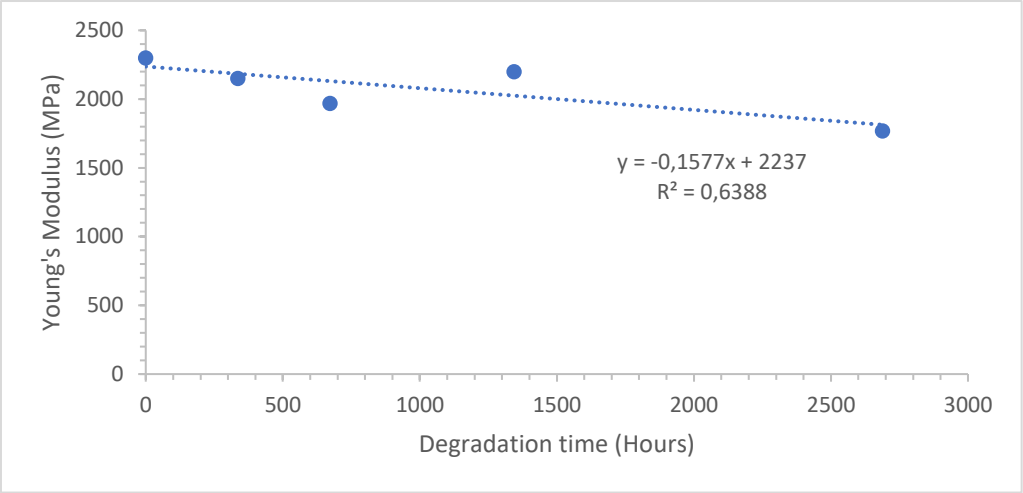

Figure 335 - Regression model used for the Young's Modulus of PLA-PCL

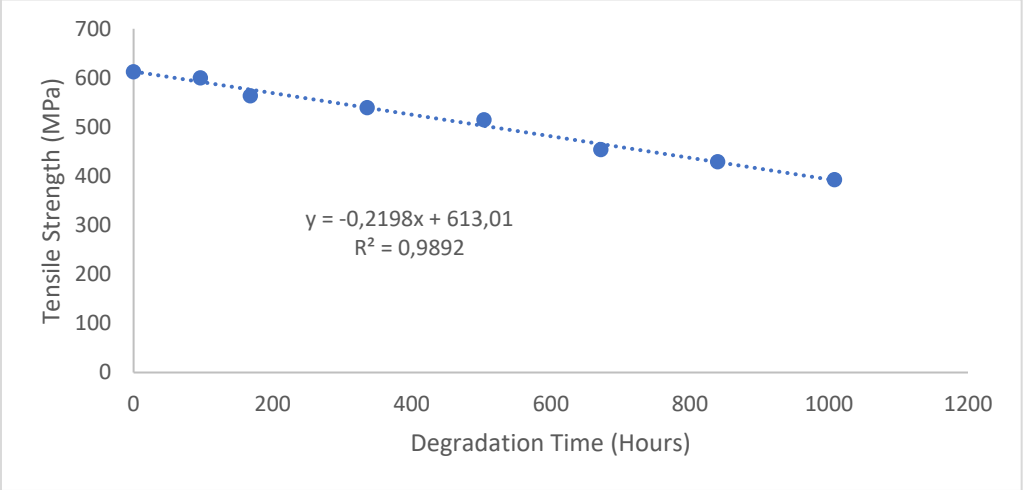

Figure 4 - Regression model used for the Tensile strength of PDS

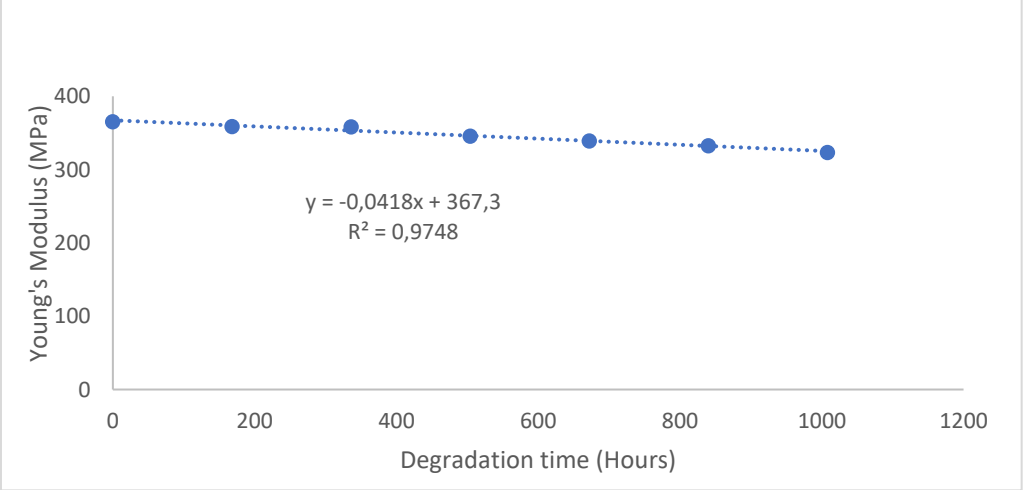

Figure 5 - Regression model used for the Young's Modulus of PDS

Annex B - Diagram of the procedure used in the simulations in the Isostrain and Isostress conditions

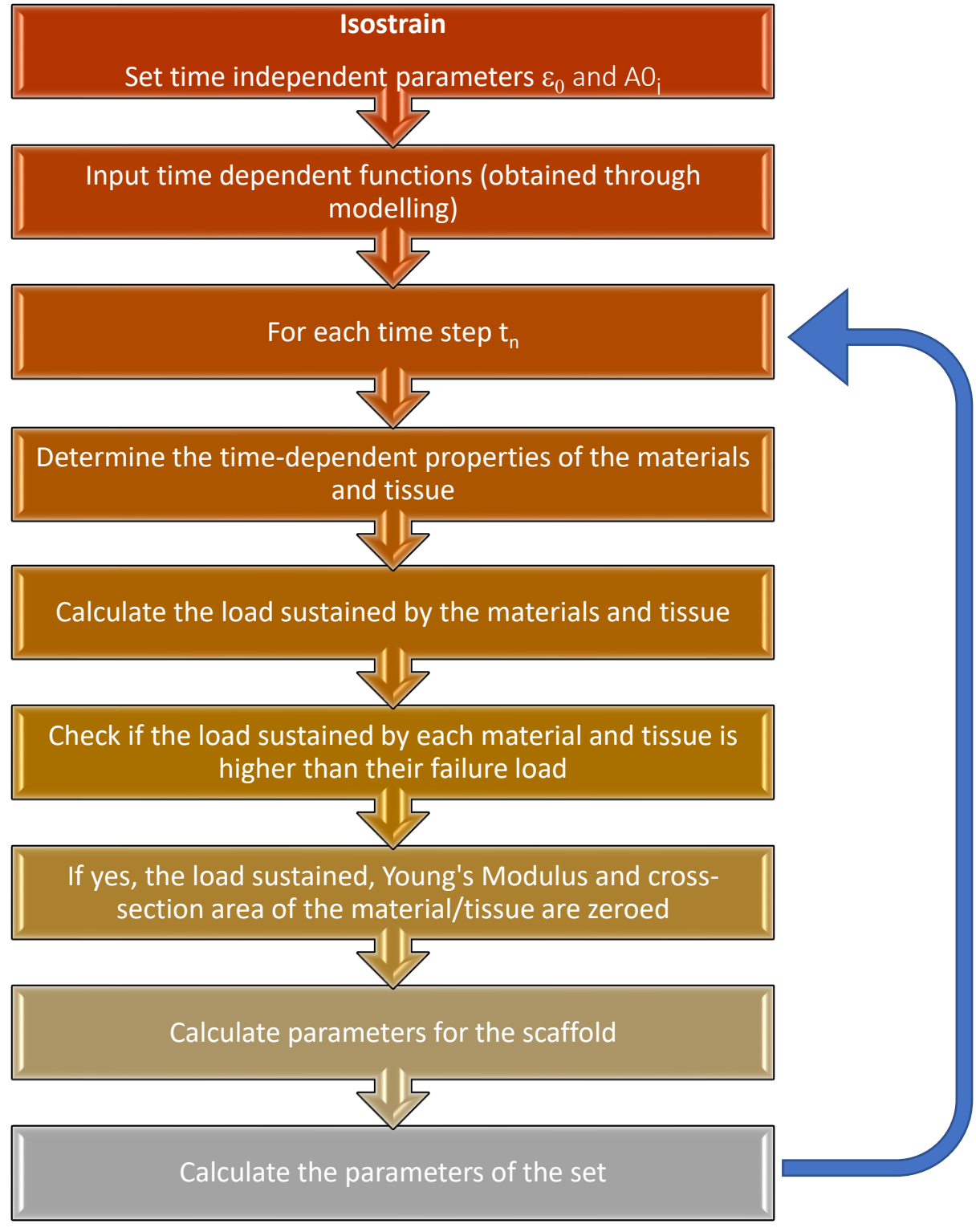

Figure 1 - Diagram illustrating the algorithmic procedure followed in the isostrain condition

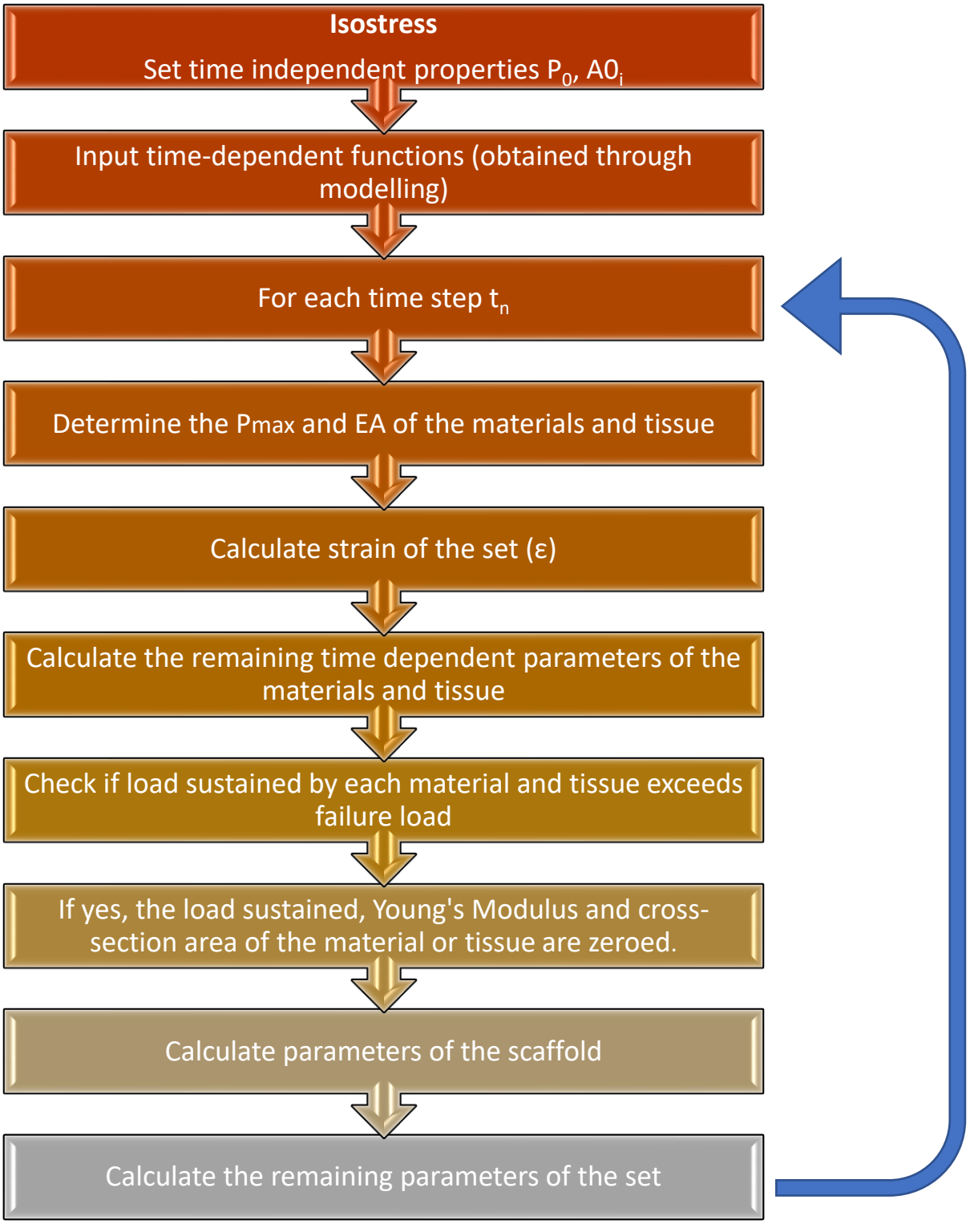

Figure 2 - Diagram illustrating the algorithmic procedure followed in the isostress condition